

Efficient RF Chain Selection for MIMO Integrated Sensing and Communications: A Greedy Approach

Subin Shin, Seongkyu Jung, Jinseok Choi, and Jeonghun Park

Abstract—In multiple-input multiple-output integrated sensing and communication (MIMO ISAC) systems, radio frequency chain (i.e., RF chain) selection plays a vital role in reducing hardware cost, power consumption, and computational complexity. However, designing an effective RF chain selection strategy is challenging due to the disparity in performance metrics between communication and sensing—mutual information (MI) versus beam-pattern mean-squared error (MSE) or the Cramér-Rao lower bound (CRLB). To overcome this, we propose a low-complexity greedy RF chain selection framework maximizing a unified MI-based performance metric applicable to both functions. By decomposing the total MI into individual contributions of each RF chain, we introduce two approaches: greedy eigen-based selection (GES) and greedy cofactor-based selection (GCS), which iteratively identify and remove the RF chains with the lowest contribution. We further extend our framework to beam selection for beamspace MIMO ISAC systems, introducing diagonal beam selection (DBS) as a simplified solution. Simulation results show that our proposed methods achieve near-optimal performance with significantly lower complexity than exhaustive search, demonstrating their practical effectiveness for MIMO ISAC systems.

I. INTRODUCTION

Integrating sensing capabilities into wireless communication systems, dubbed as integrated sensing and communication (ISAC), has been recognized as a key technology for 6G cellular networks [1]. With ISAC, it is anticipated that cellular networks enhance situational awareness, enabling more intelligent versatile communication strategies. In particular, thanks to abundant spatial degrees-of-freedom (DoF), multiple-input multiple-output (MIMO) systems facilitates both communication and sensing (i.e., MIMO radar and MIMO communications), fostering extensive research on MIMO ISAC [2].

In the context of MIMO ISAC, one of the most active research areas is transmit beamforming optimization, leveraging the well-established foundations of beamforming techniques developed for MIMO communications. For instance, in [3], [4], a semidefinite program (SDP)-based beamforming optimization method was developed under the assumption that

communication and sensing share the same hardware (antenna) and spectrum. In [5], [6], extending [3], [4], designated sensing symbols were used, wherein a joint beamforming optimization approach was proposed to minimize the mean-squared error (MSE) of the sensing beam-pattern. In [7]–[9], also considering the sensing beam-pattern MSE as the sensing performance metric as in [3]–[6], the impact of imperfect channel state information (CSI) acquisition error was taken into account in the communication performance; so as to enable the joint design of ISAC beamforming strategies. Distinct from the the sensing beam-pattern MSE mainly considered in the aforementioned studies, in [10], the Cramér-Rao lower bound (CRLB) was used as the sensing performance metric and a joint beamforming optimization method was proposed that minimizes the CRLB with given signal-to-interference-plus-noise ratio (SINR) constraints. Also, adopting the CRLB as the sensing performance metric, [11], [12] revealed the fundamental trade-off between mutual information (MI) and the CRLB (or the Fisher Information Matrix, FIM) in MIMO ISAC systems.

In addition to beamforming optimization, another critical problem for MIMO ISAC is the radio frequency (RF) chain¹ selection. As the number of RF chains increases, hardware cost, power consumption, and computational complexity also grow significantly. This makes it essential to identify a subset of RF chains that can achieve near-optimal performance [13], [14]. Motivated by this, extensive research has been conducted on RF chain selection, primarily in the context of either sensing or communication, considered separately.

In the context of sensing, several optimization techniques have been explored for addressing a sparse array beamforming problem, such as the alternating direction method of multipliers (ADMM) [15], the quadratically constrained quadratic program (QCQP) [16], and the regularization based convex relaxation [17]. Beyond the optimization based approaches, [18] developed a greedy approach that sequentially finds RF chains to minimize the CRLB, offering a computationally efficient RF chain selection strategy.

In the communication domain, there are also various RF chain selection methods in the literature. In [19], a convex relaxation method was proposed for transmit RF chain selection by relaxing a binary problem. In [20], a joint approach that combines block coordinate descent, semidefinite relaxation, and weighted minimum mean-squared error (MMSE)

¹Throughout this paper, the term RF chain is used, for simplicity, to collectively denote the hardware path and its connected antenna(s), following the convention in antenna/RF chain selection literature. For consistency, we refer to antenna selection techniques in prior work as RF chain selection.

This work was supported by Institute of Information & communications Technology Planning & Evaluation (IITP) grant funded by the Korea government(MSIT) (No. RS-2024-00395824, Development of Cloud virtualized RAN (vRAN) system supporting upper-midband), in part by Institute of Information & communications Technology Planning & Evaluation (IITP) grant funded by the Korea government(MSIT) (No. RS-2024-00397216, Development of the Upper-mid Band Extreme massive MIMO(E-MIMO)). S. Shin, S. Jung and J. Park are with the School of Electrical and Electronic Engineering, Yonsei University, South Korea (e-mail:sbshin@yonsei.ac.kr, wjdtjd963@yonsei.ac.kr, jhpark@yonsei.ac.kr). J. Choi is with the School of Electrical Engineering, Korea Advanced Institute of Science and Technology (KAIST), South Korea (e-mail:jinseok@kaist.ac.kr).

was developed to handle binary selection variables. However, these convex relaxation-based methods typically require to use off-the-shelf optimization tools like CVX, leading to extremely high computational complexity [21]. To reduce computational complexity, in [14], [22]–[24], sequential RF chain selection techniques were proposed. In these approaches, the sum capacity is decomposed into multiple components, each corresponding to the contribution of the RF chain to the overall capacity. Correspondingly, this decomposition enables a greedy selection process with significantly reduced computational burden. Building upon the decomposition technique developed in [14], [22]–[24], a joint precoding and beam selection strategy was investigated in [25] for a beamspace MIMO system. In [26], [27], the decomposition framework was extended to incorporate the effect of low-resolution quantizers, allowing the RF chain selection process to account for quantization-induced distortion.

Despite its importance, however, RF chain selection in MIMO ISAC systems has received relatively limited attention. In [28], a dynamic programming-based optimization framework was used to identify candidate RF chain subsets; thereafter the transmit covariance matrix was optimized based on the selected RF chain subset. In [29], the ADMM combined with majorization-minimization (MM) was applied to jointly optimize the ISAC beamforming matrix and the RF chain selection vector. Unfortunately, existing RF chain selection methods rely on computationally intensive optimization solvers such as CVX, which limits their practical applicability and scalability. This motivates a low-complexity RF chain selection for MIMO ISAC systems.

A critical challenge for devising low-complexity RF chain selection for MIMO ISAC lies in the fundamental disparity between sensing and communication performance metrics (e.g., the beam-pattern MSE or CRLB for sensing vs. the MI for communication), which significantly complicates the design process. Interestingly, the seminal work [30] introduced the idea of using MI as an information-theoretic sensing performance metric. This concept was later extended and adopted in various studies on sensing waveform design [31]–[34]. More recently, motivated by the effectiveness of MI as a unified performance measure, the MI-based sensing metric, often referred to as sensing MI, has been widely adopted in MIMO ISAC scenarios [35]–[37]. However, to the best of our knowledge, RF chain selection for MIMO ISAC systems has not yet been investigated in the context of unified MI-based performance metrics.

In this paper, we propose low-complexity RF chain selection methods for MIMO ISAC systems, by harnessing a unified MI-based performance metric [38]. To this end, we first characterize communication MI and sensing MI, and formulate RF chain subset selection problems for both the transmit and receive sides, whose objective is to maximize the weighted sum of normalized MI. However, the optimization problem remains NP-hard, leading to prohibitively high computational complexity. To address this challenge, leveraging the fact that both sensing and communication performance metrics are expressed in terms of MI, we transform the original RF chain subset selection problem into a sequential

RF chain selection problem. To solve this, we devise two different MI decomposition-based greedy selection algorithms: greedy eigen-based selection (GES), which leverages eigenvalue decomposition (EVD) and greedy cofactor-based selection (GCS), which is based on matrix cofactor computations. Both methods decompose the overall MI into individual RF chain contributions and iteratively identify the RF chain subset by sequentially eliminating the RF chain with the lowest contribution in a greedy manner.

Further, we also show that the proposed GES and GCS are not limited to RF chain selection in fully digital architectures, but are also directly applicable to beam selection in beamspace MIMO ISAC systems with hybrid analog-digital architectures, highlighting the versatility of the proposed methods. In addition, under an asymptotic regime where the number of antennas becomes very large, we show that GCS further reduces to a simple diagonal beam selection (DBS), offering an alternative with even lower computational complexity.

Through extensive numerical results, we demonstrate that the proposed methods outperform baseline approaches. In particular, we demonstrate that the proposed algorithms consistently achieve near-optimal performance across a wide range of average signal-to-noise ratio (SNR) values and the number of active RF chains. Notably, the proposed methods also yield considerable energy efficiency gains. These gains come from the fact that a carefully selected subset of RF chains can capture most of the ISAC system performance, thereby reducing unnecessary circuit power consumption. Finally, by illustrating the Pareto boundary, we demonstrate that the proposed methods achieve a desirable balance between communication and sensing objectives.

The rest of the paper is organized as follows. Section II models the considered system and formulates the transmit RF chain selection problem. Section III proposes GES and GCS to solve the formulated problem and demonstrates their applicability to the receive RF chain selection problem. Section IV illustrates how our proposed methods can be readily applied in the beamspace domain and demonstrates the reduction of GCS to simplified DBS in asymptotic cases. Section V validates the performance of the proposed methods through extensive numerical results. Section VI concludes the paper.

Notations: Boldface uppercase and lowercase letters denote matrices and vectors (e.g., \mathbf{A} , \mathbf{a}), respectively. $[\mathbf{A}]_{i,:}$, $[\mathbf{A}]_{:,j}$, and $[\mathbf{A}]_{i,j}$ denote the i -th row, j -th column, and (i, j) -th entry of \mathbf{A} , while \mathbf{A}_{ij} denotes a submatrix. \mathbf{I}_N denotes the $N \times N$ identity matrix. Superscripts $(\cdot)^H$, $(\cdot)^T$, $(\cdot)^{-1}$ denote Hermitian, transpose, and inversion; $\mathbf{A}^{-H} = (\mathbf{A}^H)^{-1}$. $\mathcal{A} = \{a_1, \dots, a_n\}$ denotes a set, and \mathcal{A}^c its complement. $|\cdot|$ denotes determinant for matrices and cardinality for sets. The operator $\text{diag}(\cdot)$ creates a diagonal matrix from a vector or extracts diagonal entries from a matrix. \mathbb{C} , \mathbb{R} and \mathbb{B} denote the complex numbers, real numbers and binary field, respectively.

II. SYSTEM MODEL

We consider the MIMO ISAC system in which a base station (BS) with N_t antennas simultaneously communicates with a user equipment (UE) and performs target sensing. Specifically,

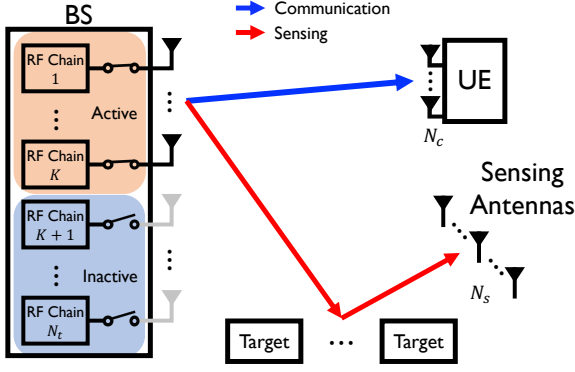


Fig. 1. The considered bistatic MIMO ISAC system with K selected RF chains.

for communication, we assume that the UE is equipped with N_c antennas. For sensing, we assume a bistatic setup as in [11], where the N_s sensing antennas are located separately from the BS. In all cases, we consider a uniform linear array (ULA) configuration, where each antenna is connected to a dedicated RF chain. Therefore, selecting RF chains directly corresponds to antenna selection in this configuration. Fig. 1 illustrates the considered system.

A. Channel and Target Response Model

Now we describe the communication channel from the BS to the UE. The communication channel matrix is given as

$$\mathbf{H}_c = \sum_{\ell=1}^L a_{c,\ell} \mathbf{r}(\phi_\ell^c) \mathbf{t}^H(\theta_\ell^c) \in \mathbb{C}^{N_c \times N_t}, \quad (1)$$

where L is the number of paths, $a_{c,\ell} \in \mathbb{C}$ is the attenuation coefficient of ℓ -th path drawn from $\mathcal{CN}(0, 1)$. $\mathbf{t}(\theta_\ell^c) \in \mathbb{C}^{N_t}$ and $\mathbf{r}(\phi_\ell^c) \in \mathbb{C}^{N_c}$ are transmit and receive array response vector, respectively. Under half-wavelength spacing, $\mathbf{t}(\theta_\ell^c)$ and $\mathbf{r}(\phi_\ell^c)$ are given as

$$\mathbf{t}(\theta_\ell^c) = [1, e^{-j\pi \sin \theta_\ell^c}, \dots, e^{-j\pi(N_t-1) \sin \theta_\ell^c}]^T, \quad (2)$$

$$\mathbf{r}(\phi_\ell^c) = [1, e^{-j\pi \sin \phi_\ell^c}, \dots, e^{-j\pi(N_c-1) \sin \phi_\ell^c}]^T, \quad (3)$$

where θ_ℓ^c and ϕ_ℓ^c are the angle of departure (AoD) and angle of arrival (AoA) of ℓ -th path, respectively.

Now we model the sensing target response matrix (TRM). Following the assumption of [33], we consider that sensing antennas are widely separated. In this case, to model the target response from n -th target to sensing antennas, we define $[\bar{\mathbf{r}}_n]_{i,:} = (d_{in})^{-\rho/2} e^{-j2\pi \frac{d_{in}}{\lambda}}$, where d_{in} denotes the distance between n -th target and i -th sensing antenna. Here, λ , ρ are the wavelength of carrier frequency, path-loss exponent, respectively. The term $(d_{in})^{-\rho/2}$ captures the path-loss induced by d_{in} . Using $\bar{\mathbf{r}}_n$ and assuming the number of target is the same as the number of sensing antennas, we express the TRM from the BS to the sensing antennas as follows:

$$\mathbf{H}_s = \sum_{n=1}^{N_s} a_{s,n} \bar{\mathbf{r}}_n \mathbf{t}^H(\theta_n^s) \in \mathbb{C}^{N_s \times N_t}, \quad (4)$$

where $a_{s,n} \in \mathbb{C} \sim \mathcal{CN}(0, (\sigma_n^s)^2)$ is the complex reflection coefficient. We note that this follows Swerling-I model [39].

In (1) and (4), it is assumed that all transmit RF chains are used. To represent a case where a specific subset of RF transmit RF chains of size K is used, we first define the index set of active transmit RF chains as $\mathcal{N}_t = \{n_1, \dots, n_K\}$ and $|\mathcal{N}_t| = K$. Then, we further denote the corresponding selection matrix as

$$\mathbf{S}(\mathcal{N}_t) = [\mathbf{e}_{n_1}, \mathbf{e}_{n_2}, \dots, \mathbf{e}_{n_K}] \in \mathbb{B}^{N_t \times K}, \quad (5)$$

where $\mathbf{e}_n \in \mathbb{B}^{N_t}$ is the n -th standard basis vector in which the n -th entry is one and all other entries are zeros. Using the selection matrix $\mathbf{S}(\mathcal{N}_t)$, we denote the channel and TRM corresponding to \mathcal{N}_t as follows:

$$\mathbf{H}_c(\mathcal{N}_t) = \mathbf{H}_c \mathbf{S}(\mathcal{N}_t) \in \mathbb{C}^{N_c \times K}, \quad (6)$$

$$\mathbf{H}_s(\mathcal{N}_t) = \mathbf{H}_s \mathbf{S}(\mathcal{N}_t) \in \mathbb{C}^{N_s \times K}. \quad (7)$$

B. Signal Model

Following [40], we denote the transmit signal at time slot t as $\mathbf{x}(t) = [x_1(t), \dots, x_{N_t}(t)]^T \in \mathbb{C}^{N_t}$ and assume that $\mathbf{x}(t) \sim \mathcal{CN}(\mathbf{0}, P\mathbf{I}_{N_t})$ with the average transmit power P . Accordingly, we denote the transmit signal during T time slots as $\mathbf{X} = [\mathbf{x}(1), \dots, \mathbf{x}(T)] \in \mathbb{C}^{N_t \times T}$. Considering transmit RF chain selection, we write the transmit signal as

$$\mathbf{X}(\mathcal{N}_t) = \mathbf{S}^T(\mathcal{N}_t) \mathbf{X} \in \mathbb{C}^{K \times T}. \quad (8)$$

Subsequently, the received signal at the communication UE during T time slots is written as

$$\mathbf{Y}_c(\mathcal{N}_t) = \mathbf{H}_c(\mathcal{N}_t) \mathbf{X}(\mathcal{N}_t) + \mathbf{Z}_c \in \mathbb{C}^{N_c \times T}, \quad (9)$$

where $\mathbf{Z}_c \in \mathbb{C}^{N_c \times T}$ is the noise during T time slots, where each column is independently and identically distributed (i.i.d.) as $\mathcal{CN}(\mathbf{0}, \sigma_c^2 \mathbf{I}_{N_c})$ with σ_c^2 representing the variance of communication noise.

Similarly, the received signal at sensing antennas during T time slots is

$$\mathbf{Y}_s^H(\mathcal{N}_t) = \mathbf{X}^H(\mathcal{N}_t) \mathbf{H}_s^H(\mathcal{N}_t) + \mathbf{Z}_s^H \in \mathbb{C}^{T \times N_s}, \quad (10)$$

where $\mathbf{Z}_s^H \in \mathbb{C}^{T \times N_s}$ is the noise during T time slots, where each column is drawn from i.i.d. Gaussian $\mathcal{CN}(\mathbf{0}, \sigma_s^2 \mathbf{I}_T)$ with σ_s^2 representing the variance of sensing noise. For notational simplicity, we assume that the variance of the communication and the sensing noise are identical and denote them by σ^2 . Furthermore, we denote the average transmit power-to-noise ratio $\frac{P}{\sigma^2}$ by γ .

C. Performance Metrics and Problem Formulation

We explain the performance metrics and formulate the problem. In the communication system, the MI between the received signal at communication UE ($\mathbf{Y}_c(\mathcal{N}_t)$) and the transmit signal ($\mathbf{X}(\mathcal{N}_t)$) conditioned on the communication channel ($\mathbf{H}_c(\mathcal{N}_t)$) is used to measure the achievable rate [41].

Accordingly, based on (9), we present the communication MI as

$$I_c(\mathcal{N}_t) = I(\mathbf{X}(\mathcal{N}_t); \mathbf{Y}_c(\mathcal{N}_t) | \mathbf{H}_c(\mathcal{N}_t)) \\ = T \log_2 \left| \mathbf{I}_K + \gamma \mathbf{H}_c^H(\mathcal{N}_t) \mathbf{H}_c(\mathcal{N}_t) \right|, \quad (11)$$

$$= T \log_2 \left| \mathbf{I}_{N_c} + \gamma \mathbf{H}_c(\mathcal{N}_t) \mathbf{H}_c^H(\mathcal{N}_t) \right|, \quad (12)$$

where (12) is the result of applying the Weinstein-Aronszajn identity $|\mathbf{I} + \mathbf{AB}| = |\mathbf{I} + \mathbf{BA}|$.

For the sensing system, we adopt the sensing MI as the sensing performance metric, defined as the MI between the received signal ($\mathbf{Y}_s(\mathcal{N}_t)$) and the TRM ($\mathbf{H}_s(\mathcal{N}_t)$) conditioned on the transmit signal ($\mathbf{X}(\mathcal{N}_t)$). As presented in [37], the sensing MI closely resembles the form of communication MI, which often makes joint optimization more tractable. Moreover, it is analytically linked to conventional sensing metrics such as the MSE and CRLB. For further details, we refer the reader to [41].

As shown in [11], [37], when the number of time slots T is sufficiently large (i.e., $T \gg N_s$), which is typical in communication scenarios, it is reasonable to approximate the sample covariance matrix of the transmit signal as

$$\frac{1}{T} \mathbf{X}(\mathcal{N}_t) \mathbf{X}^H(\mathcal{N}_t) \approx \mathbb{E}[\mathbf{X}(\mathcal{N}_t) \mathbf{X}^H(\mathcal{N}_t)] = \mathbf{P} \mathbf{I}_K. \quad (13)$$

Modeling that the columns of $\mathbf{H}_c^H(\mathcal{N}_t)$ are independent as in [33], the sensing MI based on (10) is obtained as

$$I_s(\mathcal{N}_t) = \sum_{n=1}^{N_s} \log_2 \left| \mathbf{I}_K + \frac{1}{\sigma^2} \mathbf{R}_{T,n}(\mathcal{N}_t) \mathbf{X}(\mathcal{N}_t) \mathbf{X}^H(\mathcal{N}_t) \right|, \quad (14)$$

$$= \sum_{n=1}^{N_s} \log_2 \left| \mathbf{I}_K + \gamma T \mathbf{R}_{T,n}(\mathcal{N}_t) \right|, \quad (15)$$

where $\mathbf{R}_{T,n}(\mathcal{N}_t)$ is the covariance matrix of n -th column vector of $\mathbf{H}_s^H(\mathcal{N}_t)$, defined as

$$\mathbf{R}_{T,n}(\mathcal{N}_t) = \sum_{i=1}^{N_s} \kappa_{ni} \mathbf{S}^H(\mathcal{N}_t) \mathbf{t}(\theta_i) \mathbf{t}^H(\theta_i) \mathbf{S}(\mathcal{N}_t) \in \mathbb{C}^{K \times K}. \quad (16)$$

In (16), $\kappa_{ni} = (\sigma_i^2)^2 |\tilde{\mathbf{r}}_i|_{n,:}|^2$ captures the effect of reflection of i -th target and path loss caused by the distance between the i -th target and n -th sensing antenna.

Based on (12) and (15), we formulate the transmit RF chain selection problem that maximizes the weighted sum of normalized MI as follows:

$$\max_{\mathcal{N}_t} \quad \frac{\omega_c}{T} I_c(\mathcal{N}_t) + \frac{\omega_s}{N_s} I_s(\mathcal{N}_t) \quad (17a)$$

$$\text{s.t.} \quad |\mathcal{N}_t| = K, \quad (17b)$$

where $0 \leq \omega_c, \omega_s \leq 1$ are weights to balance the trade-off between the communication MI and the sensing MI with $\omega_c + \omega_s = 1$. In (17), note that we use the normalized communication MI and the sensing MI for tractable and balanced optimization. Correspondingly, the goal of the formulated problem is choosing the optimal subset of RF chains that maximizes the weighted sum of normalized communication MI and sensing MI. Unfortunately, (17) is an NP-hard problem that incurs prohibitively high computational complexity. In the

next section, we propose greedy RF chain selection methods that address (17) while significantly reducing computational complexity.

It is also worthwhile to mention that (17) only considers the transmit RF chain selection, whereas the receive RF chain selection is also of critical importance. In Section III-C, we investigate the receive RF chain selection problem.

III. PROPOSED RF CHAIN SELECTION METHODS

To avoid the high computational complexity arising from evaluating all possible transmit RF chain combinations, we transform (17) into a sequential transmit RF chain selection problem:

$$\max_{j \in \tilde{\mathcal{N}}_t} \quad \frac{\omega_c}{T} I_c(\tilde{\mathcal{N}}_t \cap \{j\}^c) + \frac{\omega_s}{N_s} I_s(\tilde{\mathcal{N}}_t \cap \{j\}^c), \quad (18)$$

where $\tilde{\mathcal{N}}_t$ denotes the index set of remaining transmit RF chains during the sequential selection process. We interpret the problem (18) as follows. The problem (18) aims to choose the RF chain index $j \in \tilde{\mathcal{N}}_t$ whose removal results in the minimal loss in the weighted sum of the normalized communication and sensing MI. The selection is carried out over the currently remaining transmit RF chain set $\tilde{\mathcal{N}}_t$ in a greedy fashion. After finding the optimum j^* by solving (18), the remaining RF chain set $\tilde{\mathcal{N}}_t$ is updated as $\tilde{\mathcal{N}}_t \leftarrow \tilde{\mathcal{N}}_t \cap \{j^*\}^c$ and the sequential selection process is repeated until $|\tilde{\mathcal{N}}_t| = K$.

A key step of running the greedy method for the problem (18) is sequentially finding the RF chain that has the lowest contribution to the weighted sum of the normalized sensing and communication MI. To this end, we present two different MI decomposition techniques, each corresponding to a distinct RF chain selection method: 1) GES and 2) GCS.

A. Greedy Eigen-based Selection

The GES method leverages the EVD to decompose the MI expressions. The main result underlying GES is presented in Theorem 1.

Theorem 1. Let j be an index of the RF chain included in $\tilde{\mathcal{N}}_t$ and $\mathbf{R}_{T,n} = \tilde{\mathbf{P}}_n \tilde{\Lambda}_n \tilde{\mathbf{P}}_n^H$ be the decomposition of eigenvalues. Then, communication MI and sensing MI are decomposed as follows:

$$I_c(\tilde{\mathcal{N}}_t \cap \{j\}^c) = I_c(\tilde{\mathcal{N}}_t) - T \log_2 \left((1 - \gamma \alpha_j)^{-1} \right), \quad (19)$$

$$I_s(\tilde{\mathcal{N}}_t \cap \{j\}^c) = I_s(\tilde{\mathcal{N}}_t) - \sum_{n=1}^{N_s} \log_2 \left((1 - \gamma T \beta_{n,j})^{-1} \right), \quad (20)$$

where

$$\alpha_j = \mathbf{h}_j^H \mathbf{A} \mathbf{h}_j, \quad \mathbf{h}_j = [\mathbf{H}_c]_{:,j}, \quad (21)$$

$$\mathbf{A} = \left(\mathbf{I}_{N_c} + \gamma \mathbf{H}_c(\tilde{\mathcal{N}}_t) \mathbf{H}_c^H(\tilde{\mathcal{N}}_t) \right)^{-1}, \quad (22)$$

$$\beta_{n,j} = \mathbf{g}_{n,j}^H \mathbf{B}_n \mathbf{g}_{n,j}, \quad \mathbf{g}_{n,j} = [\mathbf{G}_n^H]_{:,j}, \quad (23)$$

$$\mathbf{B}_n = \left(\mathbf{I}_r + \gamma T \mathbf{G}_n^H(\tilde{\mathcal{N}}_t) \mathbf{G}_n(\tilde{\mathcal{N}}_t) \right)^{-1}. \quad (24)$$

Additionally,

$$\mathbf{G}_n(\tilde{\mathcal{N}}_t) = \mathbf{S}^H(\tilde{\mathcal{N}}_t) \mathbf{P}_n \Lambda_n^{1/2}, \quad (25)$$

where $\mathbf{P}_n \in \mathbb{C}^{N_t \times K}$ is the submatrix of $\tilde{\mathbf{P}}_n \in \mathbb{C}^{N_t \times N_t}$, while the diagonal entries of $\Lambda_n \in \mathbb{R}^{K \times K}$ are non-zero eigenvalues of $\mathbf{R}_{T,n}$.

Proof. See Appendix A. ■

By Theorem 1, we rewrite (18) as

$$\underbrace{\frac{\omega_c}{T} I_c(\tilde{N}_t) + \frac{\omega_s}{N_s} I_s(\tilde{N}_t) - \log_2 \left((1 - \gamma \alpha_j)^{-\omega_c} \prod_{n=1}^{N_s} (1 - \gamma T \beta_{n,j})^{-\frac{\omega_s}{N_s}} \right)}_{\text{The contribution of } j\text{-th RF chain}}, \quad (26)$$

which captures the contribution of the j -th RF chain to the weighted sum of normalized MI in the considered ISAC system. To remove the RF chain with the lowest contribution at each iteration, we reformulate (18) as

$$\max_{j \in \tilde{N}_t^{(i)}} \left(1 - \gamma \alpha_j^{(i)} \right)^{\omega_c} \prod_{n=1}^{N_s} \left(1 - \gamma T \beta_{n,j}^{(i)} \right)^{\frac{\omega_s}{N_s}}, \quad (27)$$

where i denotes the current iteration number and $\alpha_j^{(i)}, \beta_{n,j}^{(i)}$ and $\tilde{N}_t^{(i)}$ are the communication and sensing contribution parameters and the index set of remaining transmit RF chains at the i -th iteration, respectively.

However, as shown in (21), (23), updating $\alpha_j^{(i)}$ and $\beta_{n,j}^{(i)}$ requires matrix inversion operations, which involve high computational complexity per iteration. To address the complexity issue, we present the following corollary, which sequentially updates $\alpha_j^{(i)}, \mathbf{A}^{(i)}$ and $\beta_{n,j}^{(i)}, \mathbf{B}_n^{(i)}$ without incurring huge computation overhead.

Corollary 1. Let $J^{(i)}$ denote the index of the RF chain that was removed at the i -th iteration. Then, $\alpha_j^{(i+1)}$ and $\beta_{n,j}^{(i+1)}$ are sequentially updated as

$$\alpha_j^{(i+1)} = \alpha_j^{(i)} + |\mathbf{h}_j^H \mathbf{a}^{(i)}|^2, \quad (28)$$

$$\beta_{n,j}^{(i+1)} = \beta_{n,j}^{(i)} + |\mathbf{g}_{n,j}^H \mathbf{b}_n^{(i)}|^2, \quad (29)$$

where

$$\mathbf{a}^{(i)} = \sqrt{\gamma \left(1 - \gamma \alpha_{J^{(i)}}^{(i)} \right)^{-1}} \mathbf{A}^{(i)} \mathbf{h}_{J^{(i)}}, \quad (30)$$

$$\mathbf{b}_n^{(i)} = \sqrt{\gamma T \left(1 - \gamma T \beta_{n,J^{(i)}}^{(i)} \right)^{-1}} \mathbf{B}_n^{(i)} \mathbf{g}_{n,J^{(i)}}. \quad (31)$$

For obtaining $\mathbf{a}^{(i+1)}$ and $\mathbf{b}_n^{(i+1)}$, $\mathbf{A}^{(i+1)}$ and $\mathbf{B}_n^{(i+1)}$ are sequentially updated as

$$\mathbf{A}^{(i+1)} = \mathbf{A}^{(i)} + \mathbf{a}^{(i)} \mathbf{a}^{(i)H}, \quad (32)$$

$$\mathbf{B}_n^{(i+1)} = \mathbf{B}_n^{(i)} + \mathbf{b}_n^{(i)} \mathbf{b}_n^{(i)H}. \quad (33)$$

Proof. See Appendix B. ■

Using Theorem 1 and Corollary 1, we develop the GES algorithm in Algorithm 1.

Algorithm 1: Greedy Eigen-based Selection

```

1 input: Desired number of RF chains  $K$ , weighting factors  $\omega_c, \omega_s$ 
2 initialize:  $i = 0, \tilde{N}_t^{(0)} = \{1, 2, \dots, N_t\}$ 
3 EVD of  $\mathbf{R}_{T,n}$ 
4 Compute  $\mathbf{A}^{(0)}, \mathbf{B}_n^{(0)}$  using (22), (24)
5 Compute  $\alpha_j^{(0)}, \beta_{n,j}^{(0)}$  using (21), (23)
6 while  $|\tilde{N}_t^{(i)}| > K$  do
7   Select  $J^{(i)}$  according to (27)
8    $\tilde{N}_t^{(i+1)} \leftarrow \tilde{N}_t^{(i)} \cap \{J^{(i)}\}^c$ 
9   if  $|\tilde{N}_t^{(i+1)}| = K$  then
10     $\mathcal{N}_t \leftarrow \tilde{N}_t^{(i+1)}$ 
11    return  $\mathcal{N}_t$ 
12  end
13  Compute  $\mathbf{a}^{(i)}, \mathbf{b}_n^{(i)}$  using (30), (31)
14  Update  $\mathbf{A}^{(i+1)}, \mathbf{B}_n^{(i+1)}$  using (32), (33)
15  Update  $\alpha_j^{(i+1)}, \beta_{n,j}^{(i+1)}$  using (28), (29)
16   $i \leftarrow i + 1$ 
17 end

```

B. Greedy Cofactor-based Selection

Similar to GES, GCS sequentially selects and removes the RF chain with the lowest contribution in a greedy fashion. In contrast to GES, the contribution of each RF chain to the weighted sum of MI is characterized by using a cofactor-based inverse matrix representation. This method follows the theorem stated below.

Theorem 2. Let j be an index of the RF chain included in \tilde{N}_t . Then, communication MI and sensing MI are decomposed as follows:

$$I_c(\tilde{N}_t \cap \{j\}^c) = I_c(\tilde{N}_t) - T \log_2(\delta_j^{-1}), \quad (34)$$

$$I_s(\tilde{N}_t \cap \{j\}^c) = I_s(\tilde{N}_t) - \sum_{n=1}^{N_s} \log_2(\varepsilon_{n,j}^{-1}) \quad (35)$$

where

$$\delta_j = [\mathbf{D}^{-1}(\tilde{N}_t)]_{j,j}, \quad (36)$$

$$\mathbf{D}(\tilde{N}_t) = \mathbf{I}_{|\tilde{N}_t|} + \gamma \mathbf{H}_c^H(\tilde{N}_t) \mathbf{H}_c(\tilde{N}_t), \quad (37)$$

$$\varepsilon_{n,j} = [\mathbf{E}_n^{-1}(\tilde{N}_t)]_{j,j}, \quad (38)$$

$$\mathbf{E}_n(\tilde{N}_t) = \mathbf{I}_{|\tilde{N}_t|} + \gamma T \mathbf{R}_{T,n}(\tilde{N}_t). \quad (39)$$

Proof. See Appendix C. ■

By Theorem 2, (18) is reformulated as

$$\max_{j \in \tilde{N}_t^{(i)}} \left(\delta_j^{(i)} \right)^{\omega_c} \prod_{n=1}^{N_s} \left(\varepsilon_{n,j}^{(i)} \right)^{\frac{\omega_s}{N_s}}, \quad (40)$$

where $\delta_j^{(i)}, \varepsilon_{n,j}^{(i)}$ are the communication and sensing contribution parameters at the i -th iteration.

Similar to GES, GCS also requires matrix inversion operations to update the parameters in each iteration. To resolve the associated computational complexity, we use the following corollary based on the Schur complement:

Algorithm 2: Greedy Cofactor-based Selection

```

1 input: Desired number of RF chains  $K$ , weighting
   factors  $\omega_c, \omega_s$ 
2 initialize:  $i = 0, \tilde{N}_t^{(0)} = \{1, 2, \dots, N_t\}$ 
3 Compute  $\mathbf{D}^{-(0)}, \mathbf{E}_n^{-(0)}$  using (37), (39)
4 Compute  $\delta_j^{(0)}, \varepsilon_{n,j}^{(0)}$  using (36), (38)
5 while  $|\tilde{N}_t^{(i)}| > K$  do
6   Select  $J^{(i)}$  according to (40)
7    $\tilde{N}_t^{(i+1)} \leftarrow \tilde{N}_t^{(i)} \cap \{J^{(i)}\}^c$ 
8   if  $|\tilde{N}_t^{(i+1)}| = K$  then
9      $\mathcal{N}_t \leftarrow \tilde{N}_t^{(i+1)}$ 
10    return  $\mathcal{N}_t$ 
11  end
12  Update  $\mathbf{D}^{-(i+1)}, \mathbf{E}_n^{-(i+1)}$  using (41), (42)
13  Update  $\delta_j^{(i+1)}, \varepsilon_{n,j}^{(i+1)}$  using (36), (38)
14   $i \leftarrow i + 1$ 
15 end

```

Corollary 2. Let $J^{(i)}$ denote the index of the RF chain that was removed at the i -th iteration. Then, $\mathbf{D}^{-(i+1)}$ and $\mathbf{E}_n^{-(i+1)}$ are sequentially updated as

$$\mathbf{D}^{-(i+1)} = \tilde{\mathbf{D}}_{11}^{-(i)} - \frac{\tilde{\mathbf{D}}_{12}^{-(i)} \tilde{\mathbf{D}}_{21}^{-(i)}}{\tilde{\mathbf{D}}_{22}^{-(i)}}, \quad (41)$$

$$\mathbf{E}_n^{-(i+1)} = \tilde{\mathbf{E}}_{n11}^{-(i)} - \frac{\tilde{\mathbf{E}}_{n12}^{-(i)} \tilde{\mathbf{E}}_{n21}^{-(i)}}{\tilde{\mathbf{E}}_{n22}^{-(i)}}, \quad (42)$$

where

$$\tilde{\mathbf{D}}^{-(i)} = \mathbf{P}^{(i)} \mathbf{D}^{-(i)} \mathbf{P}^{(i)T} = \begin{bmatrix} \tilde{\mathbf{D}}_{11}^{-(i)} & \tilde{\mathbf{D}}_{12}^{-(i)} \\ \tilde{\mathbf{D}}_{21}^{-(i)} & \tilde{\mathbf{D}}_{22}^{-(i)} \end{bmatrix}, \quad (43)$$

$$\tilde{\mathbf{E}}_n^{-(i)} = \mathbf{P}^{(i)} \mathbf{E}_n^{-(i)} \mathbf{P}^{(i)T} = \begin{bmatrix} \tilde{\mathbf{E}}_{n11}^{-(i)} & \tilde{\mathbf{E}}_{n12}^{-(i)} \\ \tilde{\mathbf{E}}_{n21}^{-(i)} & \tilde{\mathbf{E}}_{n22}^{-(i)} \end{bmatrix}, \quad (44)$$

with the permutation matrix,

$$[\mathbf{P}^{(i)}]_{k,:} = \begin{cases} \mathbf{e}_k^T & \text{for } 1 \leq k < J^{(i)} \\ \mathbf{e}_{k+1}^T & \text{for } J^{(i)} \leq k < |\tilde{N}_t^{(i)}| \\ \mathbf{e}_{J^{(i)}}^T & \text{for } k = |\tilde{N}_t^{(i)}| \end{cases}. \quad (45)$$

Proof. See Appendix D. \blacksquare

Using Theorem 2 and Corollary 2, we develop the GCS algorithm in Algorithm 2.

Remark 1. GES and GCS are distinguished by the fundamental operations they leverage to evaluate and select RF chains. Specifically, GES leverages EVD to decompose the MI expressions, providing a detailed understanding of the structure of the covariance matrix. On the other hand, GCS leverages a cofactor-based inverse matrix representation to analyze the matrix structure without explicitly extracting rank information.

C. Receive RF chain Selection

Now we explore the receive RF chain selection. In the considered MIMO ISAC system, the receive RF chain selection is more simpler compared to the transmit RF chain selection because the communication MI and the sensing MI are inherently decoupled at the receiver side. As a result, receive RF chain selection is independently performed at each communication UE and sensing antennas separately without complicated interdependence between the two domains.

Denoting the active communication and sensing receive RF chain sets as $\mathcal{N}_c = \{n_{c,1}, \dots, n_{c,K}\}$ and $\mathcal{N}_s = \{n_{s,1}, \dots, n_{s,K}\}$, respectively, we rewrite the communication MI (12) and sensing MI (15) in terms of \mathcal{N}_c and \mathcal{N}_s as follows:

$$I_c(\mathcal{N}_c) = T \log_2 \left| \mathbf{I}_{N_t} + \gamma \mathbf{H}_c^H(\mathcal{N}_c) \mathbf{H}_c(\mathcal{N}_c) \right|, \quad (46)$$

$$= T \log_2 \left| \mathbf{I}_K + \gamma \mathbf{H}_c(\mathcal{N}_c) \mathbf{H}_c^H(\mathcal{N}_c) \right|, \quad (47)$$

$$I_s(\mathcal{N}_s) = \sum_{n \in \mathcal{N}_s} \log_2 \left| \mathbf{I}_{N_t} + \gamma \mathbf{T} \mathbf{R}_{T,n} \right|, \quad (48)$$

where

$$\mathbf{H}_c(\mathcal{N}_c) = \mathbf{S}_r^T(\mathcal{N}_c) \mathbf{H}_c \in \mathbb{C}^{K \times N_t}, \quad (49)$$

$$\mathbf{S}_r(\mathcal{N}_c) = [\mathbf{e}_{n_{s,1}}, \mathbf{e}_{n_{s,2}}, \dots, \mathbf{e}_{n_{s,K}}] \in \mathbb{B}^{N_c \times K}. \quad (50)$$

In (47) and (48), we observe that the communication MI and the sensing MI are affected only by their own respective receive RF chain sets. Therefore, the sequential receive RF chain selection problem, which aims to maximize the sum of normalized MI, are formulated as two independent optimization problems as follows:

$$\max_{j \in \mathcal{N}_c} \frac{1}{T} I_c(\tilde{\mathcal{N}}_c \cap \{j\}^c), \quad (51a)$$

$$\max_{j \in \mathcal{N}_s} \frac{1}{N_s} I_s(\tilde{\mathcal{N}}_s \cap \{j\}^c). \quad (51b)$$

For the communication receive RF chain selection (51a), we observe that (46) and (47) have the equivalent form as (12) and (11), respectively, in terms of how RF chain removal is represented in the equations. For this reason, we can apply (46) to Theorem 1 and Corollary 1. Similarly, (47) can be applied to Theorem 2 and Corollary 2. Accordingly, it is possible to directly apply the GES and GCS methods to solve (51a). Due to space limitations, we omit the detailed explanation.

Meanwhile, the sensing RF chain selection (51b) is even more simpler compared to the communication counterpart. To be specific, the contribution of n -th sensing RF chain to the sensing MI is explicitly expressed as $\log_2 |\mathbf{I}_{N_t} + \gamma \mathbf{T} \mathbf{R}_{T,n}|$. Consequently, (51b) is reformulated as

$$\max_{n \in \mathcal{N}_s} \left| \mathbf{I}_{N_t} + \gamma \mathbf{T} \mathbf{R}_{T,n} \right|, \quad (52)$$

which is straightforward to solve by calculating and comparing $|\mathbf{I}_{N_t} + \gamma \mathbf{T} \mathbf{R}_{T,n}|$ for all candidate sensing RF chains $n \in \mathcal{N}_s$.

IV. EXTENSION TO BEAM SELECTION FOR HYBRID MIMO ISAC ARCHITECTURE

In the previous sections, we develop the GES and GCS algorithms under the assumption that each RF chain is connected to a single antenna, thereby focusing specifically on

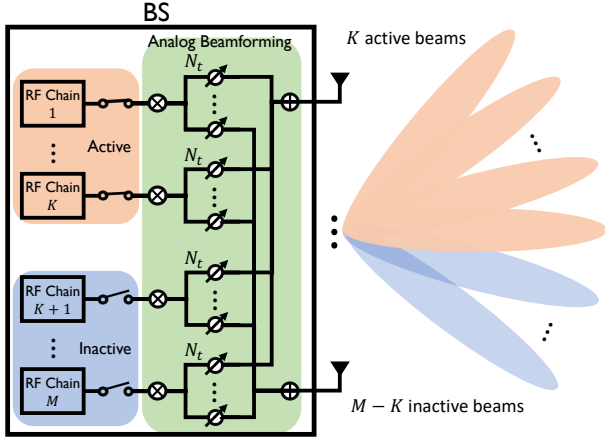


Fig. 2. Beam selection with K active RF chains. Orang beams represent the selected (active) beams, while blue beams represent unselected (inactive) beams.

RF chain selection. In this section, we extend our proposed methods to hybrid beamforming architecture [42], wherein each RF chain is connected to N_t antennas via dedicated phase shifters. Within this architecture, the original problem of RF chain selection naturally evolves into beam selection. Especially, each RF chain is associated with a distinct beam-pattern generated through a particular configuration of phase shifters.

Specifically, we consider a setup with M RF chains, where each connected to all N_t antennas through individual phase shifters as shown in Fig. 2. By tuning these phase shifters appropriately, each RF chain synthesizes a beamformed signal as a linear combination of signals from all N_t antennas. Consequently, each RF chain explicitly corresponds to a unique beam-pattern derived from this combination of antenna signals. Assuming that analog beamforming is fixed and designed to divide the angular domain into M evenly spaced beams [14], we represent the beamforming vector for the m -th RF chain as follows:

$$\mathbf{u}_m = \sqrt{\frac{1}{N_t}} \left[1, e^{-j2\pi \frac{m-1}{M}}, \dots, e^{-j2\pi (N_t-1) \frac{m-1}{M}} \right]^T \in \mathbb{C}^{N_t}. \quad (53)$$

These beams are formed by uniformly selecting columns from the $N_t \times N_t$ unitary discrete Fourier transform (DFT) matrix to divide the angular domain into M equal parts. We denote the analog beamforming matrix by $\mathbf{U} = [\mathbf{u}_1, \dots, \mathbf{u}_M] \in \mathbb{C}^{N_t \times M}$.

Under the assumption of using \mathbf{U} , the received signals at communication UE and sensing antennas (9), (10) are reformulated as

$$\mathbf{Y}_c = \tilde{\mathbf{H}}_c \tilde{\mathbf{X}} + \mathbf{Z}_c, \quad (54)$$

$$\mathbf{Y}_s^H = \tilde{\mathbf{X}}^H \tilde{\mathbf{H}}_s^H + \mathbf{Z}_s^H, \quad (55)$$

where

$$\tilde{\mathbf{H}}_c = \mathbf{H}_c \mathbf{U} \in \mathbb{C}^{N_c \times M}, \quad (56)$$

$$\tilde{\mathbf{H}}_s^H = \mathbf{U}^H \mathbf{H}_s^H \in \mathbb{C}^{M \times N_s}. \quad (57)$$

Note that $\tilde{\mathbf{X}} \in \mathbb{C}^{M \times T}$ represents the signal from the RF chains, not the signals transmitted from the antennas. $\tilde{\mathbf{H}}_c$, $\tilde{\mathbf{H}}_s^H$ are

effective channel and TRM combined with the analog beamforming matrix. As a result, the covariance matrix for each column of the effective TRM is defined as $\tilde{\mathbf{R}}_{T,n} = \mathbf{U}^H \mathbf{R}_{T,n} \mathbf{U}$.

Based on the above received signals, communication MI (11) and sensing MI (15) are rewritten as

$$I_c(\mathcal{M}) = T \log_2 \left| \mathbf{I}_M + \gamma \tilde{\mathbf{H}}_c^H(\mathcal{M}) \tilde{\mathbf{H}}_c(\mathcal{M}) \right|, \quad (58)$$

$$I_s(\mathcal{M}) = \sum_{n=1}^{N_s} \log_2 \left| \mathbf{I}_M + \gamma T \tilde{\mathbf{R}}_{T,n}(\mathcal{M}) \right|, \quad (59)$$

where $\mathcal{M} = \{1, \dots, M\}$ is the entire RF chain set. Note that the above equations have the same form as the (11) and (15). By substituting $\tilde{\mathbf{H}}_c(\mathcal{M})$ and $\tilde{\mathbf{R}}_{T,n}(\mathcal{M})$ for $\mathbf{H}_c(N_t)$ and $\mathbf{R}_{T,n}(N_t)$ in (11) and (15), respectively, and adjusting the size of the identity matrix, the previously established theorems and corollaries remain applicable. In this way, the proposed GES and GCS methods can be used without loss of generality.

It is worth noting that under the following asymptotic conditions:

- $M \rightarrow N_t$,
- $N_t \rightarrow \infty$ and $N_c \rightarrow \infty$,
- $\{\theta_\ell^c\}_{\ell=1}^L$ and $\{\phi_\ell^c\}_{\ell=1}^L$ are pairwise distinct,

the MI expressions (58) and (59) become significantly simplified. Recall the communication channel (1) and the covariance of each column vector of \mathbf{H}_s^H (16). When the above asymptotic conditions hold, $\{\mathbf{t}(\theta_\ell^c)\}_{\ell=1}^L$, $\{\mathbf{r}(\phi_\ell^c)\}_{\ell=1}^L$ and $\{\mathbf{t}(\theta_n^s)\}_{n=1}^{N_s}$ become orthogonal [43] and $\{\mathbf{t}(\theta_\ell^c)\}_{\ell=1}^L$ and $\{\mathbf{t}(\theta_n^s)\}_{n=1}^{N_s}$ align closely with exactly one analog beamforming vector of \mathbf{U} [42]. As a result, the columns of $\tilde{\mathbf{H}}_c(\mathcal{M})$ are nearly orthogonal, so that both $\tilde{\mathbf{H}}_c^H(\mathcal{M}) \tilde{\mathbf{H}}_c(\mathcal{M})$ and $\tilde{\mathbf{R}}_{T,n}(\mathcal{M})$ become approximately diagonal matrices. Then, (58) and (59) are approximated as

$$I_c(\mathcal{M}) \approx T \log_2 |\tilde{\mathbf{D}}(\mathcal{M})| = \sum_{j=1}^M T \log_2 \tilde{d}_j, \quad (60)$$

$$I_s(\mathcal{M}) \approx \sum_{n=1}^{N_s} \log_2 |\tilde{\mathbf{E}}_n(\mathcal{M})| = \sum_{j=1}^M \sum_{n=1}^{N_s} \log_2 \tilde{e}_{n,j}, \quad (61)$$

where

$$\begin{aligned} \tilde{\mathbf{D}}(\mathcal{M}) &= \text{diag} \left(\mathbf{I}_M + \gamma \tilde{\mathbf{H}}_c^H(\mathcal{M}) \tilde{\mathbf{H}}_c(\mathcal{M}) \right) \\ &= \text{diag}([\tilde{d}_1, \dots, \tilde{d}_M]^T), \end{aligned} \quad (62)$$

$$\begin{aligned} \tilde{\mathbf{E}}_n(\mathcal{M}) &= \text{diag} \left(\mathbf{I}_M + \gamma T \tilde{\mathbf{R}}_{T,n}(\mathcal{M}) \right) \\ &= \text{diag}([\tilde{e}_{n,1}, \dots, \tilde{e}_{n,M}]^T). \end{aligned} \quad (63)$$

Note that (60) and (61) correspond to Theorem 2 under the asymptotic case. Specifically, δ_j and $\varepsilon_{n,j}$ in Theorem 2 reduce to

$$\delta_j = [\tilde{\mathbf{D}}^{-1}(\mathcal{M})]_{j,j} = \tilde{d}_j^{-1}, \quad (64)$$

$$\varepsilon_{n,j} = [\tilde{\mathbf{E}}^{-1}(\mathcal{M})]_{j,j} = \tilde{e}_{n,j}^{-1}. \quad (65)$$

Building upon this derivation, the contributions of the j -th RF chain to the communication MI and sensing MI are expressed as $T \log_2 \tilde{d}_j$ and $\sum_{n=1}^{N_s} \log_2 \tilde{e}_{n,j}$, respectively, which are equivalent to (60) and (61). In GES and GCS, the contribution of each RF chain is computed via computationally expensive

Algorithm 3: Diagonal Beam Selection

- 1 **input:** Desired number of RF chains K , weighting factors ω_c, ω_s
 - 2 Compute $\tilde{\mathbf{D}}, \tilde{\mathbf{E}}_n$
 - 3 Compute $\tilde{d}_j, \tilde{e}_{n,j}$
 - 4 Compute contributions $(\tilde{d}_j)^{\omega_c} \left(\prod_{n=1}^{N_s} \tilde{e}_{n,j} \right)^{\frac{\omega_s}{N_s}}$
 - 5 Select K RF chains with the lowest contribution
 - 6 **return** $\mathcal{M} \leftarrow$ indices of selected RF chains
-

matrix inversion, which requires sequential updates to avoid full recomputation at each iteration (recall Corollaries 1 and 2). In contrast, in this case, contributions are obtained simply by extracting the diagonal entries of the matrices $\tilde{\mathbf{D}}(\mathcal{M})$ and $\tilde{\mathbf{E}}_n(\mathcal{M})$. Furthermore, these contributions remain unchanged throughout the selection process, eliminating the need for any sequential update. As a result, it is possible to select the desired number of RF chains in a single step rather than sequentially, which further reduces the computational complexity.

We refer to this special case as diagonal beam selection (DBS) and the corresponding selection procedure is summarized in Algorithm 3. Although DBS is developed under the assumption that the aforementioned asymptotic conditions hold, we demonstrate in Section V that it still achieves competitive performance even when these conditions are not satisfied.

V. NUMERICAL RESULTS

In this section, we evaluate the performance of the proposed RF chain selection algorithms. In the simulations, we consider the MIMO ISAC system with hybrid architecture, where a single RF chain is connected to N_t antennas with particular phase shifters. In such a setup, we first select K_c receive RF chains from N_c and K_s receive RF chains from N_s . Then, with given receive RF chains, we subsequently perform transmit RF chain selection. Specifically, we select K RF chains from M based on the previously selected receive RF chains.

As baselines for comparison, we consider the following methods.

- **Full-Selection:** All available RF chains at BS, communication UE and sensing antennas are used without any selection process.
- **Exhaustive Search (Exh):** Exhaustively search all combinations of K_c and K_s receive RF chains from N_c and N_s , respectively, and select the one maximizing the weighted sum of normalized MI. Then, given the selected receive RF chains, select K transmit RF chains from M in the same manner.
- **Random Selection (Random):** Transmit RF chains at the BS and receive RF chains at both the communication UE and sensing antennas are randomly selected.
- **Fixed RF chain Selection (Fixed):** Transmit and receive RF chains are pre-determined by uniformly sampling with fixed spacing and rounding. For example, when $K = 4$ and $M = 8$, the selected transmit RF chains are $\mathcal{M} = \{1, 3, 5, 7\}$.

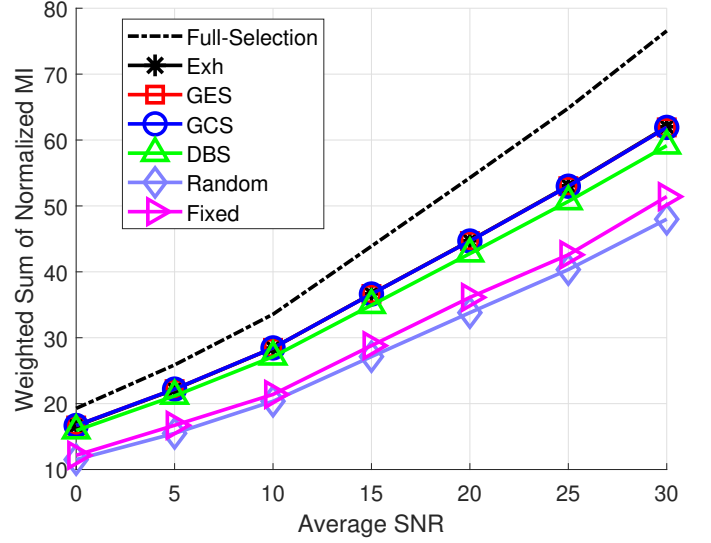


Fig. 3. The weighted sum of normalized MI over average SNR (dB) in beamspace. The number of paths, antennas at BS, RF chains at BS, UE, sensing side are set to $L = 8$, $N_t = 16$, $M = 16$, $N_c = 8$, $N_s = 8$, $K = 8$, $K_c = K_s = 6$, respectively. The communication and sensing weights are $\omega_c = 0.5$, $\omega_s = 0.5$.

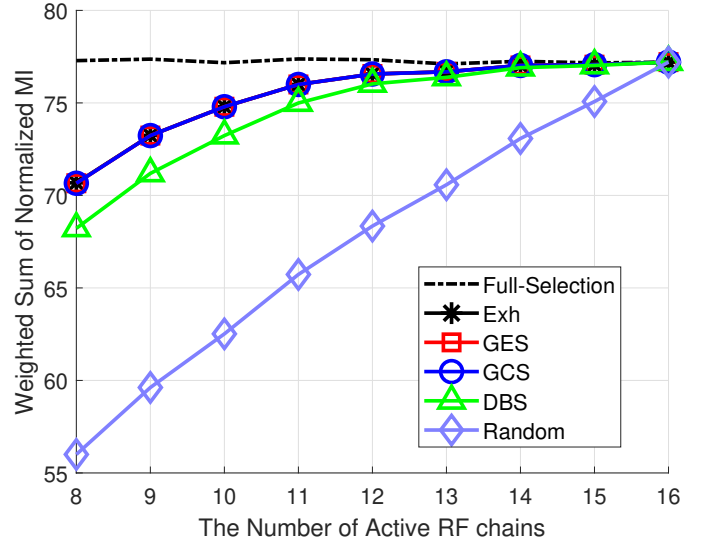


Fig. 4. The weighted sum of normalized MI over the number of active RF chains in beamspace. The number of paths, RF chains at BS, UE, sensing side are set to $L = 8$, $N_t = 16$, $N_c = 8$, $N_s = 8$, $K_c = K_s = 8$, respectively. The communication and sensing weights are $\omega_c = 0.5$, $\omega_s = 0.5$ and average SNR are set to 30dB.

The simulation environment follows the communication channel and TRM models described in Section II. The communication UE and sensing targets are randomly distributed within the angular sector $[-\pi/3, \pi/3]$. That is to say, for UE and each target located at angle θ , the corresponding AoD is uniformly distributed over $[\theta - \pi/3, \theta + \pi/3]$.

A. Weighted Sum of Normalized MI

In this subsection, we evaluate the weighted sum of normalized MI achieved by the proposed methods and baselines as a function of average SNR and the number of active RF chains, respectively. The simulation configurations are described in detail in the captions of the respective figures.

Fig. 3 illustrates the weighted sum of normalized MI as a function of the average SNR. It is observed that GES and GCS exhibit performance nearly identical to Exh with indistinguishable gap, while significantly outperforming Random and Fixed at an average SNR of 20dB by 32.15% and 23.67%, respectively. To jointly enhance communication and sensing performance, RF chain selection must account for both the effective channel and the TRM. However, since each RF chain is intricately coupled with both factors, only a limited subset ends up contributing significantly to both objectives, which in turn leads to highly imbalanced contributions to the total MI across the RF chains. Accordingly, identifying RF chain subsets that account for the dominant contribution to the total MI is of critical importance. The above observations demonstrate not only the compatibility of the proposed GES and GCS with the beamspace scenario, but also their effectiveness in selecting RF chains with significant total MI contributions by accounting for the imbalanced impact of individual RF chains. It is also observed that DBS exhibits performance very close to that of GES and GCS, with a small gap of no more than 4.7% even at 30 dB. This observation suggests that DBS can achieve performance comparable to GES and GCS even when asymptotic conditions are not satisfied.

Fig. 4 illustrates the weighted sum of normalized MI as a function of the number of active RF chains. Note that we focus on the regime where more than half of the total RF chains are activated, in order to ensure that the ISAC system sufficiently leverages the available spatial DoF. For reference, the performance of Full-Selection remains unchanged with respect to the number of active RF chains, as it is equivalent to that shown in Fig. 3. The Fixed, which uses a predetermined set of RF chains regardless of the number of active RF chains, is excluded from the figure for clarity.

As shown in Fig. 4, it is observed that GES and GCS achieve performance nearly identical to that of Exh. This implies that the proposed GES and GCS methods achieve near-optimal performance, while incurring negligible performance loss in the sequential reformulation of the RF chain selection problem. We also note that DBS, despite its significantly reduced computational complexity compared to GES and GCS, achieves a performance very close to that of these more sophisticated methods. Even when the number of active RF chains is 8, which corresponds to the largest observed performance gap, the difference is only 3.57%. This demonstrates the effectiveness of DBS, striking an excellent balance between performance and implementation efficiency. In contrast, the Random exhibits poor performance except when activating nearly all RF chains, showing a 26.17% performance loss compared to GES and GCS. This notable performance degradation highlights the importance of an effective RF chain selection strategy that consistently ensures high performance across varying numbers of active RF chains.

As shown in both Fig. 3 and Fig. 4, the proposed GES and GCS achieve performance that closely matches that of Exh. Given this near-optimal performance and the prohibitive computational burden associated with Exh, we exclude it from the subsequent simulations without loss of generality. It is also worth noting that Full-Selection yields the highest

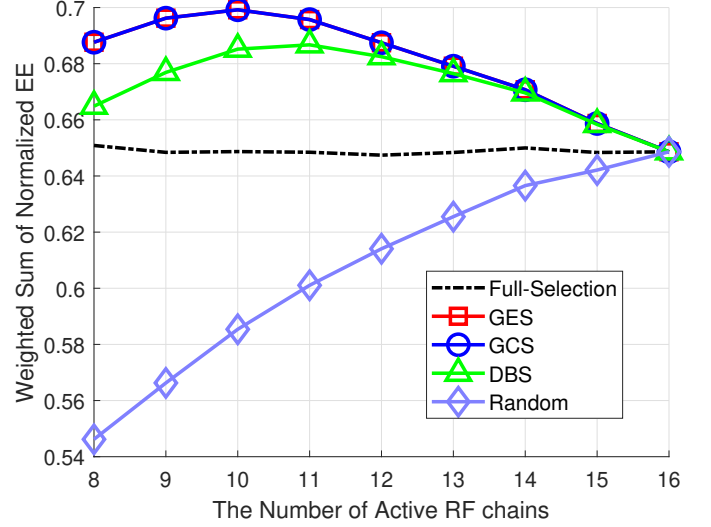


Fig. 5. The weighted sum of normalized EE over the number of active RF chains in beamspace. The number of paths, RF chains at BS, UE, and sensing side are set to $L = 8$, $N_t = 16$, $M = 16$, $N_c = 8$, $N_s = 8$, and $K_c = K_s = 8$, respectively. The communication and sensing weights are $\omega_c = 0.5$, $\omega_s = 0.5$ and the average SNR is set to 30 dB.

performance in both Fig. 3 and Fig. 4. However, it suffers from poor energy efficiency, as will be demonstrated in the next subsection.

B. Energy Efficiency

Now we examine energy efficiency (EE). To characterize normalized EE, we first consider total circuit power consumption as

$$P_{\text{cir}}(N_t, N_c, N_s) = P_{\text{BS}}(N_t) + P_{\text{UE}}(N_c) + P_s(N_s). \quad (66)$$

P_{BS} , P_{UE} , P_s are the circuit power consumption of BS, communication UE, sensing antennas, defined as

$$P_{\text{BS}}(N_t) = P_{\text{LO}} + \sum_{n \in N_t} (P_{\text{DAC}}(b_{\text{DAC},n}, f_s) + P_{\text{RF}}), \quad (67)$$

$$P_{\text{UE}}(N_c) = P_{\text{LO}} + \sum_{n \in N_c} (P_{\text{ADC}}(b_{\text{ADC},n}^c, f_s) + P_{\text{RF}}), \quad (68)$$

$$P_s(N_s) = P_{\text{LO}} + \sum_{n \in N_s} (P_{\text{ADC}}(b_{\text{ADC},n}^s, f_s) + P_{\text{RF}}), \quad (69)$$

where P_{LO} , P_{DAC} , P_{ADC} , P_{RF} , f_s denote the power consumption of local oscillator, digital-to-analog converter (DAC), analog-to-digital converter (ADC), RF chain, sampling rate, respectively. $b_{\text{DAC},n}$, $b_{\text{ADC},n}^c$, $b_{\text{ADC},n}^s$ denote quantization resolution (in bits) of n -th DAC at BS and n -th ADC at UE/sensing antennas. All parameters and power consumption functions of the DAC/ADC follow [44], [45]. We also set $b_{\text{DAC},n}$ and $b_{\text{ADC},n}^c$, $b_{\text{ADC},n}^s$ to reflect a full-resolution hardware configuration. Then, we denote the normalized EE by η , defined as follows:

$$\eta(N_t, N_c, N_s) = \frac{\frac{\omega_c}{T} I_c(N_t) + \frac{\omega_s}{N_s} I_s(N_t)}{P_{\text{cir}}(N_t, N_c, N_s)}. \quad (70)$$

Fig. 5 illustrates the weighted sum of normalized EE η of our proposed methods and baselines as a function of the number of active RF chains. Detailed simulation setups are

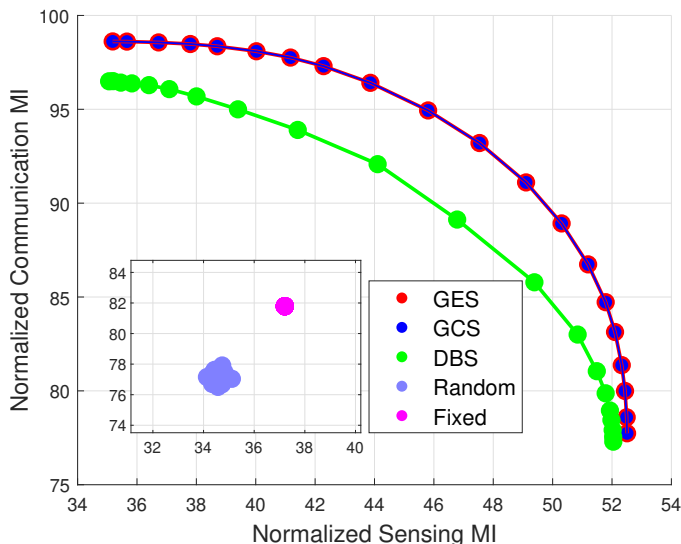


Fig. 6. The Pareto boundary of normalized communication MI and normalized sensing MI in beamspace. The number of paths, RF chains at BS, UE, sensing side are set to $L = 8$, $N_t = 16$, $M = 16$, $N_c = 8$, $N_s = 8$, $K = 8$, respectively. The average SNR are set to 30dB.

provided in the corresponding figure caption. As observed in the figure, GES, GCS and DBS achieve better EE compared to Random. This result is expected, given the performance advantages demonstrated in Fig. 4, as the proposed algorithms consume the same amount of power as Random while delivering significantly better performance. Notably, the proposed methods also outperform the Full-Selection in terms of EE, achieving up to a 7.79% improvement. This improvement is mainly due to the fact that Full-Selection activates all RF chains, resulting in significantly higher power consumption compared to the proposed methods. This suggests that fully activating all RF chains does not necessarily lead to energy-efficient operation and validates the superior EE of the proposed methods.

C. Pareto Boundary of Normalized MI

In this subsection, we plot the Pareto boundary of communication MI versus sensing MI as the weights ω_c and ω_s vary in Fig. 6. Consistent with the previous cases, the figure caption includes the detailed simulation setups. For simplicity, we do not consider receive RF chain selection in the Pareto boundary investigation. Each point on the curve in Fig. 6 represents a different weighting between communication and sensing objectives. The bottom right corresponds to $\omega_c = 0$ (sensing-only), while the top left corresponds to $\omega_c = 1$ (communication-only), with intermediate points reflecting gradual shifts in emphasis.

It is observed that the proposed GES and GCS methods achieve the best Pareto boundaries, demonstrating their superior ability to balance the trade-off between communication and sensing. It is worth noting that, while the DBS achieves performance comparable to GES and GCS in Fig. 3, Fig. 4 and Fig. 5, its corresponding Pareto boundary is relatively limited in extent.

In GCS, the key factor that determines the contribution of each RF chain is the corresponding diagonal entries of

the inverse matrix, which is influenced by the determinant of the matrix obtained by removing the corresponding row and column (see Appendix C). This determinant reflects the degree of orthogonality among the remaining channel and TRM vectors when the given RF chain is excluded. Therefore, sequentially removing the RF chain associated with the largest such determinant is equivalent to eliminating the most redundant RF chain. In contrast, DBS ignores the interdependence among RF chains captured by the off-diagonal entries and instead evaluates the contribution of each RF chain solely based on the power of its corresponding channel and TRM vectors. As a result, DBS may favor high-power yet redundant RF chains that are already well represented in either the communication or sensing subspaces. This leads to a sub-optimal selection, which fundamentally limits the overall Pareto boundary performance of DBS.

These observations collectively suggest that, when a proper balance between communication and sensing is required, the Fixed and Random are unsuitable due to their inability to account for this trade-off. While the proposed DBS method exhibits relatively better balance compared to Fixed and Random, it still falls short of providing sufficiently diverse trade-off solutions. The proposed GES and GCS consistently achieve well-balanced and widely spread Pareto boundaries, demonstrating their effectiveness as selection methods for achieving balanced performance in joint communication and sensing optimization.

VI. CONCLUSION

In this paper, we proposed two low-complexity greedy RF chain selection methods for MIMO ISAC, by harnessing a unified MI performance metric for both communication and sensing. We revealed the following key findings. First, by decomposing the MI into individual RF chain contributions, the proposed GES, GCS, and DBS algorithms enable efficient selection and achieve near-optimal performance, while significantly reducing computational complexity. Second, despite Full-Selection achieving the highest performance in terms of MI, it suffers from poor EE due to its full hardware deployment. In contrast, the proposed methods achieve better EE by judiciously selecting a subset of RF chains. Lastly, in the trade-off between communication and sensing, the proposed GES and GCS achieve the most extensive Pareto frontier, demonstrating their capability to maintain balanced performance across different weighting preferences. These findings confirm that the proposed framework offers an effective and practical solution for RF chain selection in MIMO ISAC systems.

APPENDIX A

The communication MI with \tilde{N}_t is represented as

$$I_c(\tilde{N}_t) = T \log_2 \left| \mathbf{I}_{N_c} + \gamma \mathbf{H}_c(\tilde{N}_t) \mathbf{H}_c^H(\tilde{N}_t) \right|.$$

When j -th RF chain in $\tilde{N}_t = \{n_1, \dots, n_{|\tilde{N}_t|}\}$ is removed, the corresponding j -th column of \mathbf{H}_c is also removed. Denoting

j -th column of \mathbf{H}_c by \mathbf{h}_j , we represent the communication MI as

$$\begin{aligned} I_c(\bar{\mathcal{N}}_t \cap \{j\}^c) &= T \log_2 \left| \mathbf{I}_{N_c} + \gamma \left(\mathbf{H}_c(\bar{\mathcal{N}}_t) \mathbf{H}_c^H(\bar{\mathcal{N}}_t) - \mathbf{h}_j \mathbf{h}_j^H \right) \right|, \\ &= T \log_2 \left| \left(\mathbf{I}_{N_c} + \gamma \mathbf{H}_c(\bar{\mathcal{N}}_t) \mathbf{H}_c^H(\bar{\mathcal{N}}_t) \right) - \gamma \mathbf{h}_j \mathbf{h}_j^H \right|. \end{aligned}$$

Applying determinant lemma $|\mathbf{A} + \mathbf{u}\mathbf{v}^H| = |\mathbf{A}|(1 + \mathbf{v}^H \mathbf{A}^{-1} \mathbf{u})$ to the above equation, we decompose $I_c(\bar{\mathcal{N}}_t \cap \{j\}^c)$ as follows:

$$\begin{aligned} & T \log_2 \left| \mathbf{I}_{N_c} + \gamma \mathbf{H}_c(\bar{\mathcal{N}}_t) \mathbf{H}_c^H(\bar{\mathcal{N}}_t) \right| \\ & - T \log_2 \left(\left(1 - \gamma \mathbf{h}_j^H \left(\mathbf{I}_{N_c} + \gamma \mathbf{H}_c(\bar{\mathcal{N}}_t) \mathbf{H}_c^H(\bar{\mathcal{N}}_t) \right)^{-1} \mathbf{h}_j \right) \right) \\ & \quad \underbrace{\hspace{10em}}_{\text{The contribution of } j\text{-th RF chain}} \\ & = I_c(\bar{\mathcal{N}}_t) - T \log_2 \left((1 - \gamma \alpha_j)^{-1} \right), \end{aligned}$$

where

$$\alpha_j = \mathbf{h}_j^H \mathbf{A} \mathbf{h}_j \text{ and } \mathbf{A} = (\mathbf{I}_{N_c} + \gamma \mathbf{H}_c(\bar{\mathcal{N}}_t) \mathbf{H}_c^H(\bar{\mathcal{N}}_t))^{-1}.$$

Applying EVD to $\mathbf{R}_{T,n}$ yields

$$\mathbf{R}_{T,n} = \tilde{\mathbf{P}}_n \tilde{\mathbf{\Lambda}}_n \tilde{\mathbf{P}}_n^H = \mathbf{P}_n \mathbf{\Lambda}_n \mathbf{P}_n^H = \mathbf{G}_n \mathbf{G}_n^H,$$

where the columns of $\tilde{\mathbf{P}}_n \in \mathbb{C}^{N_t \times N_t}$ are eigenvectors of $\mathbf{R}_{T,n}$ and the diagonal entries of $\tilde{\mathbf{\Lambda}}_n \in \mathbb{R}^{N_t \times N_t}$ are eigenvalues and placed in descending order. Suppose that the rank of $\mathbf{R}_{T,n}$ is r . Then, $\mathbf{R}_{T,n}$ is decomposed into $\mathbf{P}_n \in \mathbb{C}^{N_t \times r}$ and $\mathbf{\Lambda}_n \in \mathbb{R}^{r \times r}$, where \mathbf{P}_n is the submatrix of $\tilde{\mathbf{P}}_n$, while the diagonal entries of $\mathbf{\Lambda}_n$ are non-zero eigenvalues of \mathbf{R}_T . We also define \mathbf{G}_n as $\mathbf{G}_n = \mathbf{P}_n \mathbf{\Lambda}_n^{1/2} \in \mathbb{C}^{N_t \times r}$.

Then, the sensing MI $I_s(\bar{\mathcal{N}}_t)$ is expressed as

$$\begin{aligned} I_s(\bar{\mathcal{N}}_t) &= \sum_{n=1}^{N_s} I_{s,n}(\bar{\mathcal{N}}_t) = \sum_{n=1}^{N_s} \log_2 \left| \mathbf{I}_{|\bar{\mathcal{N}}_t|} + \gamma T \mathbf{R}_{T,n}(\bar{\mathcal{N}}_t) \right|, \\ &= \sum_{n=1}^{N_s} \log_2 \left| \mathbf{I}_{|\bar{\mathcal{N}}_t|} + \gamma T \mathbf{G}_n(\bar{\mathcal{N}}_t) \mathbf{G}_n^H(\bar{\mathcal{N}}_t) \right|, \\ &\stackrel{(a)}{=} \sum_{n=1}^{N_s} \log_2 \left| \mathbf{I}_r + \gamma T \mathbf{G}_n^H(\bar{\mathcal{N}}_t) \mathbf{G}_n(\bar{\mathcal{N}}_t) \right|, \end{aligned}$$

where (a) follows from Weinstein-Aronszajn identity $|\mathbf{I} + \mathbf{A}\mathbf{B}| = |\mathbf{I} + \mathbf{B}\mathbf{A}|$ and $\mathbf{G}_n(\bar{\mathcal{N}}_t)$ is $\mathbf{S}^H(\bar{\mathcal{N}}_t) \mathbf{G}_n$. $I_{s,n}(\bar{\mathcal{N}}_t)$ is the sensing MI between the received signal at n -th sensing antenna and n -th column of $\mathbf{H}_s^H(\bar{\mathcal{N}}_t)$.

When j -th RF chain of $\bar{\mathcal{N}}_t = \{n_1, \dots, n_{|\bar{\mathcal{N}}_t|}\}$ is removed, the corresponding j -th column of \mathbf{G}_n^H is also removed. Denoting j -th column of \mathbf{G}_n^H by $\mathbf{g}_{n,j}$, we formulate the n -th sensing MI as

$$I_{s,n}(\bar{\mathcal{N}}_t \cap \{j\}^c) = \log_2 \left| \mathbf{I}_r + \gamma T \left(\mathbf{G}_n^H(\bar{\mathcal{N}}_t) \mathbf{G}_n(\bar{\mathcal{N}}_t) - \mathbf{g}_{n,j} \mathbf{g}_{n,j}^H \right) \right|.$$

Applying determinant lemma to the above equation yields

$$\begin{aligned} & \log_2 \left| \mathbf{I}_r + \gamma T \mathbf{G}_n^H(\bar{\mathcal{N}}_t) \mathbf{G}_n(\bar{\mathcal{N}}_t) \right| \\ & - \log_2 \left(\left(1 - \gamma T \mathbf{g}_{n,j}^H \left(\mathbf{I}_r + \gamma T \mathbf{G}_n^H(\bar{\mathcal{N}}_t) \mathbf{G}_n(\bar{\mathcal{N}}_t) \right)^{-1} \mathbf{g}_{n,j} \right) \right) \\ & \quad \underbrace{\hspace{10em}}_{\text{The } n\text{-th contribution of } j\text{-th RF chain}} \\ & = I_{s,n}(\bar{\mathcal{N}}_t) - \log_2 \left((1 - \gamma T \beta_{n,j})^{-1} \right), \end{aligned}$$

where

$$\beta_{n,j} = \mathbf{g}_{n,j}^H \mathbf{B}_n \mathbf{g}_{n,j} \text{ and } \mathbf{B}_n = \left(\mathbf{I}_r + \gamma T \mathbf{G}_n^H(\bar{\mathcal{N}}_t) \mathbf{G}_n(\bar{\mathcal{N}}_t) \right)^{-1}.$$

Therefore, total sensing MI $I_s(\bar{\mathcal{N}}_t \cap \{j\}^c)$ is decomposed as follows:

$$I_s(\bar{\mathcal{N}}_t \cap \{j\}^c) = I_s(\bar{\mathcal{N}}_t) - \sum_{n=1}^{N_s} \log_2 \left((1 - \gamma T \beta_{n,j})^{-1} \right).$$

APPENDIX B

For ease of exposition, we denote i -th remaining RF chain set as $\bar{\mathcal{N}}_t^{(i)}$. According to this notation, we additionally denote $\mathbf{H}_c^{(i)} = \mathbf{H}_c(\bar{\mathcal{N}}_t^{(i)}) = \mathbf{H}_c \mathbf{S}(\bar{\mathcal{N}}_t^{(i)})$ and $\mathbf{G}_n^{(i)} = \mathbf{G}_n(\bar{\mathcal{N}}_t^{(i)}) = \mathbf{S}^H(\bar{\mathcal{N}}_t^{(i)}) \mathbf{G}_n$.

Assuming that the RF chain with the lowest contribution is removed, $\mathbf{A}^{(i+1)}$ is rewritten as

$$\begin{aligned} \mathbf{A}^{(i+1)} &= \left(\mathbf{I}_{N_c} + \gamma \mathbf{H}_c^{(i+1)} \mathbf{H}_c^{(i+1)H} \right)^{-1} \\ &= \left(\underbrace{\mathbf{I}_{N_c} + \gamma \mathbf{H}_c^{(i)} \mathbf{H}_c^{(i)H}}_{(\mathbf{A}^{(i)})^{-1}} - \gamma \mathbf{h}_{J(i)} \mathbf{h}_{J(i)}^H \right)^{-1}. \end{aligned}$$

Applying Woodbury matrix identity $(\mathbf{A} + \mathbf{UCV})^{-1} = \mathbf{A}^{-1} - \mathbf{A}^{-1} \mathbf{U} (\mathbf{C}^{-1} + \mathbf{V} \mathbf{A}^{-1} \mathbf{U})^{-1} \mathbf{V} \mathbf{A}^{-1}$ to the above equation yields

$$\begin{aligned} & \mathbf{A}^{(i)} + \gamma \mathbf{A}^{(i)} \mathbf{h}_{J(i)} \left(1 - \gamma \mathbf{h}_{J(i)}^H \mathbf{A}^{(i)} \mathbf{h}_{J(i)} \right)^{-1} \mathbf{h}_{J(i)}^H \mathbf{A}^{(i)}, \\ & = \mathbf{A}^{(i)} + \gamma \left(1 - \gamma \alpha_{J(i)}^{(i)} \right)^{-1} \mathbf{A}^{(i)} \mathbf{h}_{J(i)} \mathbf{h}_{J(i)}^H \mathbf{A}^{(i)} = \mathbf{A}^{(i)} + \mathbf{a}^{(i)} \mathbf{a}^{(i)H}, \end{aligned}$$

where $\mathbf{a}^{(i)} \triangleq \sqrt{\gamma \left(1 - \gamma \alpha_{J(i)}^{(i)} \right)^{-1}} \mathbf{A}^{(i)} \mathbf{h}_{J(i)}$.

Note that, since $\mathbf{A}^{(i+1)}$ consists of $\mathbf{A}^{(i)}$ and $\mathbf{a}^{(i)}$ which are obtained at previous iteration, $\mathbf{A}^{(i+1)}$ can be sequentially updated easily. For the same reason, $\alpha_j^{(i+1)}$ for all $j \in \bar{\mathcal{N}}_t^{(i+1)}$ are sequentially updated as

$$\begin{aligned} \alpha_j^{(i+1)} &= \mathbf{h}_j^H \mathbf{A}^{(i+1)} \mathbf{h}_j = \mathbf{h}_j^H \left(\mathbf{A}^{(i)} + \mathbf{a}^{(i)} \mathbf{a}^{(i)H} \right) \mathbf{h}_j, \\ &= \alpha_j^{(i)} + |\mathbf{h}_j^H \mathbf{a}^{(i)}|^2. \end{aligned}$$

In the same way, $\mathbf{B}_n^{(i+1)}, \beta_{n,j}^{(i)}$ also can be sequentially updated as follows:

$$\begin{aligned} \mathbf{B}_n^{(i+1)} &= \left(\mathbf{I}_r + \gamma T \mathbf{G}_n^{(i+1)H} \mathbf{G}_n^{(i+1)} \right)^{-1} \\ &= \left(\underbrace{\mathbf{I}_r + \gamma T \mathbf{G}_n^{(i)H} \mathbf{G}_n^{(i)}}_{(\mathbf{B}_n^{(i)})^{-1}} - \gamma T \mathbf{g}_{n,J(i)} \mathbf{g}_{n,J(i)}^H \right)^{-1}, \\ &= \mathbf{B}_n^{(i)} + \gamma T \left(1 - \gamma T \beta_{n,J(i)}^{(i)} \right)^{-1} \mathbf{B}_n^{(i)} \mathbf{g}_{n,J(i)} \mathbf{g}_{n,J(i)}^H \mathbf{B}_n^{(i)}, \\ &= \mathbf{B}_n^{(i)} + \mathbf{b}_n^{(i)} \mathbf{b}_n^{(i)H}, \end{aligned}$$

where $\mathbf{b}_n^{(i)} \triangleq \sqrt{\gamma T \left(1 - \gamma T \beta_{n,J(i)}^{(i)} \right)^{-1}} \mathbf{B}_n^{(i)} \mathbf{g}_{n,J(i)}$ and

$$\begin{aligned} \beta_{n,j}^{(i+1)} &= \mathbf{g}_{n,j}^H \mathbf{B}_n^{(i+1)} \mathbf{g}_{n,j} = \mathbf{g}_{n,j}^H \left(\mathbf{B}_n^{(i)} + \mathbf{b}_n^{(i)} \mathbf{b}_n^{(i)H} \right) \mathbf{g}_{n,j}, \\ &= \beta_{n,j}^{(i)} + |\mathbf{g}_{n,j}^H \mathbf{b}_n^{(i)}|^2. \end{aligned}$$

APPENDIX C

The communication MI with $\tilde{\mathcal{N}}_t$ is represented as

$$I_c(\tilde{\mathcal{N}}_t) = T \log_2 \left| \mathbf{I}_{|\tilde{\mathcal{N}}_t|} + \gamma \mathbf{H}_c^H(\tilde{\mathcal{N}}_t) \mathbf{H}_c(\tilde{\mathcal{N}}_t) \right| = T \log_2 |\mathbf{D}(\tilde{\mathcal{N}}_t)|,$$

where we denote $\mathbf{I}_{|\tilde{\mathcal{N}}_t|} + \gamma \mathbf{H}_c^H(\tilde{\mathcal{N}}_t) \mathbf{H}_c(\tilde{\mathcal{N}}_t)$ by $\mathbf{D}(\tilde{\mathcal{N}}_t)$. When j -th RF chain of $\tilde{\mathcal{N}}_t = \{n_1, \dots, n_{|\tilde{\mathcal{N}}_t|}\}$ is removed, the corresponding j -th row and column of $\mathbf{D}(\tilde{\mathcal{N}}_t)$ are also removed, and this matrix is denoted by $\mathbf{D}(\tilde{\mathcal{N}}_t \cap \{j\}^c)$. By representing $\mathbf{D}^{-1}(\tilde{\mathcal{N}}_t)$ in terms of adjugate matrix of $\mathbf{D}(\tilde{\mathcal{N}}_t)$ [46], its (j, j) -th entry is expressed as

$$[\mathbf{D}^{-1}(\tilde{\mathcal{N}}_t)]_{j,j} = \frac{C_{jj}}{|\mathbf{D}(\tilde{\mathcal{N}}_t)|} = \frac{|\mathbf{D}(\tilde{\mathcal{N}}_t \cap \{j\}^c)|}{|\mathbf{D}(\tilde{\mathcal{N}}_t)|},$$

where $C_{jj} = (-1)^{(2j)} |\mathbf{D}(\tilde{\mathcal{N}}_t \cap \{j\}^c)|$ is cofactor of $[\mathbf{D}(\tilde{\mathcal{N}}_t)]_{j,j}$. Therefore, we represent the communication MI with $\tilde{\mathcal{N}}_t \cap \{j\}^c$ as

$$\begin{aligned} I_c(\tilde{\mathcal{N}}_t \cap \{j\}^c) &= T \log_2 |\mathbf{D}(\tilde{\mathcal{N}}_t \cap \{j\}^c)|, \\ &= T \log_2 |\mathbf{D}(\tilde{\mathcal{N}}_t)| - \underbrace{T \log_2 \left([\mathbf{D}^{-1}(\tilde{\mathcal{N}}_t)]_{j,j}^{-1} \right)}_{\text{The contribution of } j\text{-th RF chain}}, \\ &= I_c(\tilde{\mathcal{N}}_t) - T \log_2 \left(\delta_j^{-1} \right), \end{aligned}$$

where $\delta_j = [\mathbf{D}^{-1}(\tilde{\mathcal{N}}_t)]_{j,j}$.

In the same way, denoting $|\mathbf{I}_{|\tilde{\mathcal{N}}_t|} + \gamma T \mathbf{R}_{T,n}(\tilde{\mathcal{N}}_t)|$ as $\mathbf{E}_n(\tilde{\mathcal{N}}_t)$, sensing MI with $\tilde{\mathcal{N}}_t \cap \{j\}^c$ is represented as

$$\begin{aligned} I_s(\tilde{\mathcal{N}}_t \cap \{j\}^c) &= \sum_{n=1}^{N_s} \log_2 |\mathbf{E}_n(\tilde{\mathcal{N}}_t \cap \{j\}^c)|, \\ &= \sum_{n=1}^{N_s} \log_2 |\mathbf{E}_n(\tilde{\mathcal{N}}_t)| - \underbrace{\sum_{n=1}^{N_s} \log_2 \left([\mathbf{E}_n^{-1}(\tilde{\mathcal{N}}_t)]_{j,j}^{-1} \right)}_{\text{The contribution of } j\text{-th RF chain}}, \\ &= I_s(\tilde{\mathcal{N}}_t) - \sum_{n=1}^{N_s} \log_2 \left(\varepsilon_{n,j}^{-1} \right), \end{aligned}$$

where $\varepsilon_{n,j} = [\mathbf{E}_n^{-1}(\tilde{\mathcal{N}}_t)]_{j,j}$.

APPENDIX D

For ease of exposition, we denote i -th remaining RF chain set by $\tilde{\mathcal{N}}_t^{(i)}$. According to this notation, we additionally denote $\mathbf{D}^{(i)} = \mathbf{D}(\tilde{\mathcal{N}}_t^{(i)})$ and $\mathbf{E}_n^{(i)} = \mathbf{E}_n(\tilde{\mathcal{N}}_t^{(i)})$.

To enable the sequential update of inverse of $\mathbf{D}^{(i+1)}$ and $\mathbf{E}_n^{(i+1)}$, we leverage the Schur complement. To facilitate this process, an appropriate row permutation matrix is defined as follows:

$$[\mathbf{P}^{(i)}]_{k,:} = \begin{cases} \mathbf{e}_k^T & \text{for } 1 \leq k < J^{(i)} \\ \mathbf{e}_{k+1}^T & \text{for } J^{(i)} \leq k < |\tilde{\mathcal{N}}_t^{(i)}|, \\ \mathbf{e}_{J^{(i)}}^T & \text{for } k = |\tilde{\mathcal{N}}_t^{(i)}| \end{cases}$$

where $\mathbf{e}_k \in \mathbb{R}^{|\tilde{\mathcal{N}}_t^{(i)}|}$ is the k -th standard basis vector in which the k -th entry is one and all other entries are zeros. This matrix moves $J^{(i)}$ -th row to the last row (i.e., $|\tilde{\mathcal{N}}_t^{(i)}|$ -th position), and shifts the rows from $(J^{(i)} + 1)$ -th to $|\tilde{\mathcal{N}}_t^{(i)}|$ upward by

one position, i.e., to rows $J^{(i)}$ -th to $(|\tilde{\mathcal{N}}_t^{(i)}| - 1)$, respectively. The corresponding column permutation can be applied by multiplying with the transpose of the row permutation matrix from the right.

The matrix $\mathbf{D}^{(i)}$ permuted on both rows and columns by $\mathbf{P}^{(i)}$ and $\mathbf{P}^{(i)T}$ is defined as

$$\tilde{\mathbf{D}}^{(i)} \triangleq \mathbf{P}^{(i)} \mathbf{D}^{(i)} \mathbf{P}^{(i)T} = \begin{bmatrix} \mathbf{D}^{(i+1)} & \mathbf{d}_{J^{(i)}} \\ \mathbf{d}_{J^{(i)}}^H & d_{J^{(i)}J^{(i)}} \end{bmatrix}.$$

By using Schur complement of $d_{J^{(i)}J^{(i)}}$, we obtain the inverse of $\tilde{\mathbf{D}}^{(i)}$ as

$$\tilde{\mathbf{D}}^{-(i)} = \mathbf{P}^{(i)} \mathbf{D}^{-(i)} \mathbf{P}^{(i)T} = \begin{bmatrix} \tilde{\mathbf{D}}_{11}^{-(i)} & \tilde{\mathbf{D}}_{12}^{-(i)} \\ \tilde{\mathbf{D}}_{21}^{-(i)} & \tilde{\mathbf{D}}_{22}^{-(i)} \end{bmatrix},$$

where

$$\begin{aligned} \tilde{\mathbf{D}}_{11}^{-(i)} &= \left(\tilde{\mathbf{D}}^{(i)} / d_{J^{(i)}J^{(i)}} \right)^{-1} \in \mathbb{C}^{|\tilde{\mathcal{N}}_t^{(i+1)}| \times |\tilde{\mathcal{N}}_t^{(i+1)}|}, \\ \tilde{\mathbf{D}}_{12}^{-(i)} &= - \left(\tilde{\mathbf{D}}^{(i)} / d_{J^{(i)}J^{(i)}} \right)^{-1} \frac{\mathbf{d}_{J^{(i)}}}{d_{J^{(i)}J^{(i)}}} \in \mathbb{C}^{|\tilde{\mathcal{N}}_t^{(i+1)}|}, \\ \tilde{\mathbf{D}}_{21}^{-(i)} &= - \frac{\mathbf{d}_{J^{(i)}}^H}{d_{J^{(i)}J^{(i)}}} \left(\tilde{\mathbf{D}}^{(i)} / d_{J^{(i)}J^{(i)}} \right)^{-1} \in \mathbb{C}^{1 \times |\tilde{\mathcal{N}}_t^{(i+1)}|}, \\ \tilde{\mathbf{D}}_{22}^{-(i)} &= \frac{1}{d_{J^{(i)}J^{(i)}}} + \frac{\mathbf{d}_{J^{(i)}}^H \left(\tilde{\mathbf{D}}^{(i)} / d_{J^{(i)}J^{(i)}} \right)^{-1} \mathbf{d}_{J^{(i)}}}{|d_{J^{(i)}J^{(i)}}|^2} \in \mathbb{C}, \end{aligned}$$

and

$$\tilde{\mathbf{D}}^{(i)} / d_{J^{(i)}J^{(i)}} = \mathbf{D}^{(i+1)} - \frac{\mathbf{d}_{J^{(i)}} \mathbf{d}_{J^{(i)}}^H}{d_{J^{(i)}J^{(i)}}}$$

is Schur complement of $d_{J^{(i)}J^{(i)}}$.

Since $\tilde{\mathbf{D}}^{(i)}$ is the inverse of $\tilde{\mathbf{D}}^{-(i)}$, $\tilde{\mathbf{D}}^{(i)}$ can be rewritten in terms of Schur complement of $\tilde{\mathbf{D}}_{22}^{-(i)}$ as

$$\begin{aligned} \tilde{\mathbf{D}}^{(i)} &= \begin{bmatrix} \mathbf{S}_{\tilde{\mathbf{D}}_{22}^{-(i)}}^{-1} & -\mathbf{S}_{\tilde{\mathbf{D}}_{22}^{-(i)}}^{-1} \tilde{\mathbf{D}}_{12}^{-(i)} \tilde{\mathbf{D}}_{22}^{-(i)} \\ -\mathbf{D}^{-1} \tilde{\mathbf{D}}_{21}^{-(i)} \mathbf{S}_{\tilde{\mathbf{D}}_{22}^{-(i)}}^{-1} & \mathbf{S}_{\tilde{\mathbf{D}}_{22}^{-(i)}} + \tilde{\mathbf{D}}_{22}^{-(i)} \tilde{\mathbf{D}}_{21}^{-(i)} \mathbf{S}_{\tilde{\mathbf{D}}_{22}^{-(i)}}^{-1} \tilde{\mathbf{D}}_{12}^{-(i)} \tilde{\mathbf{D}}_{22}^{-(i)} \end{bmatrix}, \end{aligned}$$

where $\mathbf{S}_{\tilde{\mathbf{D}}_{22}^{-(i)}} = \tilde{\mathbf{D}}^{(i)} / \tilde{\mathbf{D}}_{22}^{-(i)}$ is Schur complement of $\tilde{\mathbf{D}}_{22}^{-(i)}$.

Thus, $\mathbf{D}^{(i+1)} = \mathbf{S}_{\tilde{\mathbf{D}}_{22}^{-(i)}}^{-1}$ and we obtain $\mathbf{D}^{-(i+1)}$ as

$$\mathbf{D}^{-(i+1)} = \mathbf{S}_{\tilde{\mathbf{D}}_{22}^{-(i)}} = \tilde{\mathbf{D}}_{11}^{-(i)} - \frac{\tilde{\mathbf{D}}_{12}^{-(i)} \tilde{\mathbf{D}}_{21}^{-(i)}}{\tilde{\mathbf{D}}_{22}^{-(i)}}.$$

Since $\tilde{\mathbf{D}}_{11}^{-(i)}$, $\tilde{\mathbf{D}}_{12}^{-(i)}$, $\tilde{\mathbf{D}}_{21}^{-(i)}$, $\tilde{\mathbf{D}}_{22}^{-(i)}$ are already obtained by permuting on both rows and columns of $\mathbf{D}^{-(i)}$, we sequentially update $\mathbf{D}^{-(i+1)}$ without inversion operation.

In the same way, $\mathbf{E}_n^{(i+1)}$, $\mathbf{E}_n^{-(i+1)}$ are obtained as

$$\tilde{\mathbf{E}}_n^{(i)} \triangleq \mathbf{P}^{(i)} \mathbf{E}_n^{(i)} \mathbf{P}^{(i)T} = \begin{bmatrix} \mathbf{E}_n^{(i+1)} & \mathbf{f}_{n,J^{(i)}} \\ \mathbf{f}_{n,J^{(i)}}^H & e_{n,J^{(i)}J^{(i)}} \end{bmatrix},$$

$$\tilde{\mathbf{E}}_n^{-(i)} = \mathbf{P}^{(i)} \mathbf{E}_n^{-(i)} \mathbf{P}^{(i)T} = \begin{bmatrix} \tilde{\mathbf{E}}_{n11}^{-(i)} & \tilde{\mathbf{E}}_{n12}^{-(i)} \\ \tilde{\mathbf{E}}_{n21}^{-(i)} & \tilde{\mathbf{E}}_{n22}^{-(i)} \end{bmatrix},$$

$$\mathbf{E}_n^{-(i+1)} = \tilde{\mathbf{E}}_{n11}^{-(i)} - \frac{\tilde{\mathbf{E}}_{n12}^{-(i)} \tilde{\mathbf{E}}_{n21}^{-(i)}}{\tilde{\mathbf{E}}_{n22}^{-(i)}}.$$

REFERENCES

- [1] F. Liu, Y. Cui, C. Masouros, J. Xu, T. X. Han, Y. C. Eldar, and S. Buzzi, "Integrated sensing and communications: Toward dual-functional wireless networks for 6g and beyond," *IEEE J. Sel. Areas Commun.*, vol. 40, no. 6, pp. 1728–1767, 2022.
- [2] Y. Zhuo, T. Mao, H. Li, C. Sun, Z. Wang, Z. Han, and S. Chen, "Multi-beam integrated sensing and communication: State-of-the-art, challenges and opportunities," *IEEE Commun. Mag.*, vol. 62, no. 9, pp. 90–96, 2024.
- [3] F. Liu, C. Masouros, A. Li, H. Sun, and L. Hanzo, "MU-MIMO communications with MIMO radar: From co-existence to joint transmission," *IEEE Trans. Wireless Commun.*, vol. 17, no. 4, pp. 2755–2770, 2018.
- [4] F. Liu, L. Zhou, C. Masouros, A. Li, W. Luo, and A. Petropulu, "Toward dual-functional radar-communication systems: Optimal waveform design," *IEEE Trans. Signal Process.*, vol. 66, no. 16, pp. 4264–4279, 2018.
- [5] X. Liu, T. Huang, N. Shlezinger, Y. Liu, J. Zhou, and Y. C. Eldar, "Joint transmit beamforming for multiuser MIMO communications and MIMO radar," *IEEE Trans. Signal Process.*, vol. 68, pp. 3929–3944, 2020.
- [6] H. Hua, J. Xu, and T. X. Han, "Optimal transmit beamforming for integrated sensing and communication," *IEEE Trans. Veh. Technol.*, vol. 72, no. 8, pp. 10588–10603, 2023.
- [7] J. Choi, J. Park, N. Lee, and A. Alkhateeb, "Joint and robust beamforming framework for integrated sensing and communication systems," *IEEE Trans. Wireless Commun.*, vol. 23, no. 11, pp. 17602–17618, 2024.
- [8] N. Kim, J. Han, J. Choi, A. Alkhateeb, C.-B. Chae, and J. Park, "Integrated sensing and communications in downlink FDD MIMO without CSI feedback," *ArXiv Preprint*, 2024. [Online]. Available: <https://arxiv.org/abs/2412.12590>
- [9] N. Kim, J. Han, and J. Park, "Integrated sensing and communications in FDD MIMO without CSI feedback: Towards FDD MIMO ISAC," in *Proc. Int. Symp. on Model. and Opt. in Mobile, Ad Hoc, and Wireless Networks (WiOpt)*, 2024, pp. 132–137.
- [10] F. Liu, Y.-F. Liu, A. Li, C. Masouros, and Y. C. Eldar, "Cramér-rao bound optimization for joint radar-communication beamforming," *IEEE Trans. Signal Process.*, vol. 70, pp. 240–253, 2022.
- [11] Y. Xiong, F. Liu, Y. Cui, W. Yuan, T. X. Han, and G. Caire, "On the fundamental tradeoff of integrated sensing and communications under gaussian channels," *IEEE Trans. Inf. Theory*, vol. 69, no. 9, pp. 5723–5751, 2023.
- [12] H. Hua, T. X. Han, and J. Xu, "MIMO integrated sensing and communication: CRB-rate tradeoff," *IEEE Trans. Wireless Commun.*, vol. 23, no. 4, pp. 2839–2854, 2024.
- [13] S. Sanayei and A. Nosratinia, "Antenna selection in MIMO systems," *IEEE Commun. Mag.*, vol. 42, no. 10, pp. 68–73, 2004.
- [14] P. V. Amadori and C. Masouros, "Low RF-complexity millimeter-wave beamspace-MIMO systems by beam selection," *IEEE Trans. Commun.*, vol. 63, no. 6, pp. 2212–2223, 2015.
- [15] H. Huang, H. C. So, and A. M. Zoubir, "Sparse array beamformer design via ADMM," *IEEE Trans. Signal Process.*, vol. 71, pp. 3357–3372, 2023.
- [16] S. A. Hamza and M. G. Amin, "Hybrid sparse array beamforming design for general rank signal models," *IEEE Trans. Signal Process.*, vol. 67, no. 24, pp. 6215–6226, 2019.
- [17] X. Wang, M. S. Greco, and F. Gini, "Adaptive sparse array beamformer design by regularized complementary antenna switching," *IEEE Trans. Signal Process.*, vol. 69, pp. 2302–2315, 2021.
- [18] M. Arash, I. Stupia, and L. Vandendorpe, "Real-time CRLB based antenna selection in planar antenna arrays," *IEEE Trans. Wireless Commun.*, vol. 22, no. 6, pp. 4043–4056, 2023.
- [19] X. Gao, O. Edfors, F. Tufvesson, and E. G. Larsson, "Massive mimo in real propagation environments: Do all antennas contribute equally?" *IEEE Trans. Commun.*, vol. 63, no. 11, pp. 3917–3928, 2015.
- [20] J. M. B. d. Silva, H. Ghauch, G. Fodor, M. Skoglund, and C. Fischione, "Smart antenna assignment is essential in full-duplex communications," *IEEE Trans. Commun.*, vol. 69, no. 5, pp. 3450–3466, 2021.
- [21] J. Park, J. Choi, N. Lee, W. Shin, and H. V. Poor, "Rate-splitting multiple access for downlink MIMO: A generalized power iteration approach," *IEEE Trans. Wireless Commun.*, vol. 22, no. 3, pp. 1588–1603, 2023.
- [22] M. Gharavi-Alkhanjari and A. Gershman, "Fast antenna subset selection in MIMO systems," *IEEE Trans. Signal Process.*, vol. 52, no. 2, pp. 339–347, 2004.
- [23] B. C. Lim, W. A. Krzymien, and C. Schlegel, "Efficient sum rate maximization and resource allocation in block-diagonalized space-division multiplexing," *IEEE Trans. Veh. Technol.*, vol. 58, no. 1, pp. 478–484, 2009.
- [24] P.-H. Lin and S.-H. Tsai, "Performance analysis and algorithm designs for transmit antenna selection in linearly precoded multiuser MIMO systems," *IEEE Trans. Veh. Technol.*, vol. 61, no. 4, pp. 1698–1708, 2012.
- [25] X. Gao, L. Dai, S. Han, C.-L. I, and R. W. Heath, "Energy-efficient hybrid analog and digital precoding for mmwave MIMO systems with large antenna arrays," *IEEE J. Sel. Areas Commun.*, vol. 34, no. 4, pp. 998–1009, 2016.
- [26] J. Choi, J. Sung, N. Prasad, X.-F. Qi, B. L. Evans, and A. Gatherer, "Base station antenna selection for low-resolution ADC systems," *IEEE Trans. Commun.*, vol. 68, no. 3, pp. 1951–1965, 2020.
- [27] J. Park, S. Park, A. Yazdan, and R. W. Heath, "Optimization of mixed-ADC multi-antenna systems for cloud-RAN deployments," *IEEE Trans. Commun.*, vol. 65, no. 9, pp. 3962–3975, 2017.
- [28] M. Palaologos, M. H. Castañeda García, T. Laas, R. A. Stirling-Gallagher, and G. Caire, "Joint antenna selection and covariance matrix optimization for ISAC systems," in *Proc. IEEE Int. Conf. on Comm.*, 2024, pp. 2071–2076.
- [29] R. Liu, M. Li, and Q. Liu, "Joint transmit/receive antenna selection and beamforming design for ISAC systems," in *Proc. IEEE Glob. Comm. Conf.*, 2023, pp. 3118–3123.
- [30] M. Bell, "Information theory and radar waveform design," *IEEE Trans. Inf. Theory*, vol. 39, no. 5, pp. 1578–1597, 1993.
- [31] Y. Yang and R. S. Blum, "MIMO radar waveform design based on mutual information and minimum mean-square error estimation," *IEEE Trans. Aerosp. Electron. Syst.*, vol. 43, no. 1, pp. 330–343, 2007.
- [32] B. Tang, J. Tang, and Y. Peng, "MIMO radar waveform design in colored noise based on information theory," *IEEE Trans. Signal Process.*, vol. 58, no. 9, pp. 4684–4697, 2010.
- [33] B. Tang and J. Li, "Spectrally constrained MIMO radar waveform design based on mutual information," *IEEE Trans. Signal Process.*, vol. 67, no. 3, pp. 821–834, 2019.
- [34] G. Sun, Z. He, J. Tong, X. Yu, and S. Shi, "Mutual information-based waveform design for MIMO radar space-time adaptive processing," *IEEE Trans. Geosci. Remote Sens.*, vol. 59, no. 4, pp. 2909–2921, 2021.
- [35] C. Ouyang, Y. Liu, and H. Yang, "MIMO-ISAC: Performance analysis and rate region characterization," *IEEE Wireless Commun. Lett.*, vol. 12, no. 4, pp. 669–673, 2023.
- [36] Y. Peng, S. Yang, W. Lyu, Y. Li, H. He, Z. Zhang, and C. Assi, "Mutual information-based integrated sensing and communications: A WMMSE framework," *IEEE Wireless Commun. Lett.*, vol. 13, no. 10, pp. 2642–2646, 2024.
- [37] S. Wang, L. Chen, J. Zhou, Y. Chen, K. Han, and C. You, "Unified ISAC Pareto boundary based on mutual information and minimum mean-square error estimation," *IEEE Trans. Commun.*, vol. 72, no. 11, pp. 6783–6795, 2024.
- [38] C. Ouyang, Y. Liu, H. Yang, and N. Al-Dhahir, "Integrated sensing and communications: A mutual information-based framework," *IEEE Commun. Mag.*, vol. 61, no. 5, pp. 26–32, 2023.
- [39] P. Swerling, "Probability of detection for fluctuating targets," *IRE Trans. Inf. Theory*, vol. 6, no. 2, pp. 269–308, 1960.
- [40] P. Stoica, J. Li, and Y. Xie, "On probing signal design for MIMO radar," *IEEE Trans. Signal Process.*, vol. 55, no. 8, pp. 4151–4161, 2007.
- [41] L. Xie, F. Liu, J. Luo, and S. Song, "Sensing mutual information with random signals in gaussian channels: Bridging sensing and communication metrics," *ArXiv Preprint*, 2024. [Online]. Available: <http://arxiv.org/abs/2402.03919>
- [42] R. W. Heath, N. González-Prelcic, S. Rangan, W. Roh, and A. M. Sayeed, "An overview of signal processing techniques for millimeter wave MIMO systems," *IEEE J. Sel. Topics Signal Process.*, vol. 10, no. 3, pp. 436–453, 2016.
- [43] T. L. Marzetta, "Noncooperative cellular wireless with unlimited numbers of base station antennas," *IEEE Trans. Wireless Commun.*, vol. 9, no. 11, pp. 3590–3600, 2010.
- [44] J. Choi, J. Park, and N. Lee, "Energy efficiency maximization precoding for quantized massive MIMO systems," *IEEE Trans. Wireless Commun.*, vol. 21, no. 9, pp. 6803–6817, 2022.
- [45] S. Cui, A. Goldsmith, and A. Bahai, "Energy-constrained modulation optimization," *IEEE Trans. Wireless Commun.*, vol. 4, no. 5, pp. 2349–2360, 2005.
- [46] R. A. Horn and C. R. Johnson, *Matrix analysis*. Cambridge university press, 2012.